(Preprint) AAS 25-790

BACKSUBSTITUTION METHOD FOR PRESCRIBED MOTION ACTUATORS WITH ATTACHED DYNAMIC SUB-COMPONENTS

Leah Kiner* **and Hanspeter Schaub†**

Spacecraft systems can range from simple and compact designs to large and complex multi-body structures. For space missions with strict performance requirements and science objectives, spacecraft often contain intricate articulated components which can flex depending on the overall system dynamics. Simulation of these types of complex spacecraft systems is crucial to ensure mission success, however this nontrivial task becomes increasingly more difficult as the spacecraft system grows in size and complexity. Previous work used the backsubstitution method to separately develop the dynamics for N chained translational, rotational, and prescribed rigid bodies connected to a central rigid hub. This work expands upon prior work using the backsubstitution method to formulate the system dynamics for single and dual-axis rotating rigid bodies connected to a kinematically prescribed spacecraft component. These new developments enables a wide variety of previously impossible forking spacecraft configurations to be simulated using the backsubstitution method. A multi-body spacecraft simulation is shown to demonstrate the applicability of the derived dynamics and the hub response to the system dynamics is studied. The resulting equations of motion are verified in the appendix for both rotating rigid body derivations.

INTRODUCTION

Spacecraft simulations are critical for the success of space missions. Especially for missions that require large, complex multi-body spacecraft structures, it is crucial that simulations are representative of the true system dynamics. For example, the football-field-sized International Space Station contains a massive articulated main truss that other large components such as the space station remote manipulator system, solar panels, and experimental modules are attached to.[1] The Lucy mission ambitiously deployed two large 7.3 meter diameter flexible-substrate solar arrays using a motor-driven lanyard,[2,3] a design that will also be utilized by the Emirates Mission to the Asteroid Belt.[4–6] Similarly, the DART binary asteroid impact mission was the first of its kind to demonstrate roll-out solar array (ROSA) technology.[2,7,8] Missions to understand the evolution and environment of our neighboring planet Mars led to a plethora of advancements in robotic manipulator systems. The InSight Mars Lander was the first mission to study the interior structure of Mars, relying on a complex robotic Instrument Deployment System (IDS) containing an Instrument Deployment Arm (IDA), scoop, five finger "claw" grapple, motor controller, and several cameras to execute the scientific goals of the mission.[9] The Mars Science Laboratory (MSL) Curiosity rover uses a five-joint

*Graduate Research Assistant, Ann and H.J. Smead Department of Aerospace Engineering Sciences, University of Colorado Boulder, Colorado Center For Astrodynamics Research, Boulder, CO, 80303 USA. leah.kiner@colorado.edu

†Distinguished Professor and Department Chair, Schaden Leadership Chair, Ann and H.J. Smead Department of Aerospace Engineering Sciences, University of Colorado, Boulder, 431 UCB, Colorado Center for Astrodynamics Research, Boulder, CO, 80309. Fellow of AIAA and AAS.

five degree-of-freedom robotic arm driven by brushless DC motors for sample acquisition, processing, and delivery and to position the other scientific instruments relative to the Martian surface.[10,11] None of these ambitious missions would have been possible without incredible simulation developments for these complex spacecraft systems.

There are many different methods that can be used to derive the equations of motion for complex spacecraft systems, some of which include Newtonian mechanics, Eulerian mechanics, Lagrangian mechanics and Kane's method.[12,13] Newtonian and Eulerian mechanics are used in this work. This approach enables seamless integration with the Basilisk * astrodynamics simulation software which leverages the backsubstitution method[14–19] in order to maintain computational efficiency, modularity, and scalability of spacecraft simulations. This derivation approach is beneficial in that the resulting equations of motion are completely general and therefore can be applied to a wide range of spacecraft configurations.

The backsubstitution method is discussed in detail in Refs. [14] and [16]. The foundation of this method is the assumption of hub-centric spacecraft configurations, where all of the system bodies such as solar panels, thrusters, and antennae are attached to a central rigid core component. This assumption leads to significant computational efficiency through the unique structure of the system mass matrix for these design configurations. Deriving and back-substituting the attached component accelerations into the hub dynamics achieves a significant speed reduction because the entire system mass matrix no longer needs to be inverted. Only two 3×3 matrix inversions are required,[14] which drastically reduces the computational load.[17] For chains of rigid bodies attached to the hub and particularly forking configurations, it becomes nontrivial to derive the equations of motion for these systems because the dynamics of the entire multi-body structure connected to the hub must be derived separately and organized into the backsubstitution method. While this assumption limits the possible spacecraft design space, it ultimately encompasses a sufficiently wide spectrum of allowable spacecraft designs as has proven to adequately support several interplanetary space missions.

Prior work using the backsubstitution method has developed the equations of motion for a variety of components attached to a spacecraft hub including single-hinged solar panels,[20] reaction wheels,[21] control moment gyroscopes,[22] multi-panel solar arrays with repeated hinge axes, and linear and spherical fuel mass particles.[23] The most relevant work to the contributions of this paper is the more recent work by Carneiro et al., who developed formulations to simulate chains of both sequentially rotating rigid bodies and chains of translating rigid bodies attached to the rigid spacecraft hub.[18,24,25]

Table (1) presents the previously studied spacecraft configurations that are directly relevant to and form the basis for the contributions in this paper. Building upon these previous developments using the backsubstitution method, the single-axis and dual-axis spinner derivations in Ref. [18] are modified for attachment to prescribed motion components whose dynamics are individually derived in Ref. [19]. This work combines the dynamics of the hub and prescribed motion component system with the dynamics of the hub and rotating rigid body systems. These contributions are illustrated in Table (2), where the prescribed motion component is wedged between the spacecraft hub and spinning body systems. Not only does this work derive the dynamics for these new systems and formulate the results using the backsubstitution method, but this work also manipulates the results and groups the coupling contributions arising from these chained configurations compared to the

*https://avslab.github.io/basilisk

Table 1. Backsubstitution formulation simulation capabilities.

System	Illustration	Ref.
Hub + single-axis rotating rigid body (1-DOF spinner)	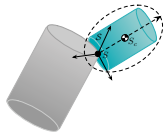	[18]
Hub + dual-axis rotating rigid body (2-DOF spinner)	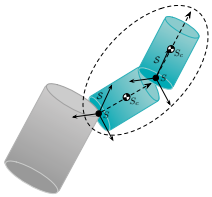	[18]
Hub + N prescribed motion components	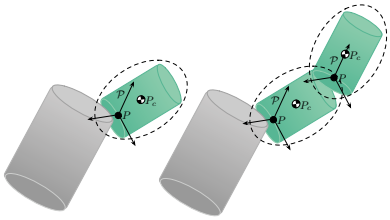	[19]

original hub-connected design derivations. The contributions of this work enable novel simulation of new forked configurations that were not previously possible using the backsubstitution method. Specifically, this work enables simulation of branching systems relative to the prescribed motion component, where previously branching was only possible relative to the spacecraft hub.

Table 2. Contributions of this work.

System	Illustration
Hub + prescribed motion component + 1-DOF spinner	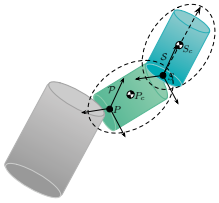
Hub + prescribed motion component + 2-DOF spinner	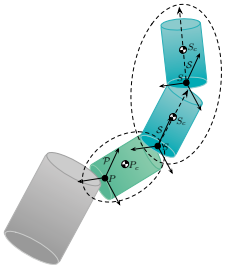

The first section of this paper derives the general equations of motion for a three-body chained spacecraft system containing a rigid hub, prescribed motion component and a single general sub-component. The results are completely general and serve as the foundation of this work. The developed equations are used in the second section as the starting point in developing the dynamics for the three-body chained system containing a single-axis rotating rigid body. The third section of this paper derives the dynamics for the same system with a dual-axis spinner rather than a single-axis spinner. Although not shown, the derivation for the dual-axis spinner system requires re-derivation of the general chained system dynamics with two general rigid bodies attached sequentially to the prescribed component. This is because the second set of general equations contains additional coupling terms between the two general rigid bodies. The following section presents a multi-body spacecraft simulation scenario using the new dual-axis formulation. The concluding remarks are offered in the final section of this paper. The equations of motion for the single and dual-axis spinner chained systems are verified using conservation principles in the appendix.

PRESCRIBED MOTION WITH ATTACHED GENERAL RIGID BODY DYNAMICS

This section derives the equations of motion for a three-body general chained system containing a general rigid body attached to a prescribed motion component. This derivation is used as the starting point to establish the equations of motion for the single-axis chained system in Sec. 2. Note that although the derivation in this section only considers a single general rigid body attached to the prescribed motion component, Sec. 3 requires a similar derivation where two general rigid bodies are attached sequentially to the prescribed motion component.

Problem Statement

Figure (1) illustrates the multi-body chained system of interest for the derivation in this section. The chained system includes a rigid hub (gray), a prescribed motion component (green), and a general rigid body with six degrees of freedom (blue). Note that while a single chain is shown, the derivation applies for N chained connections to the rigid hub.

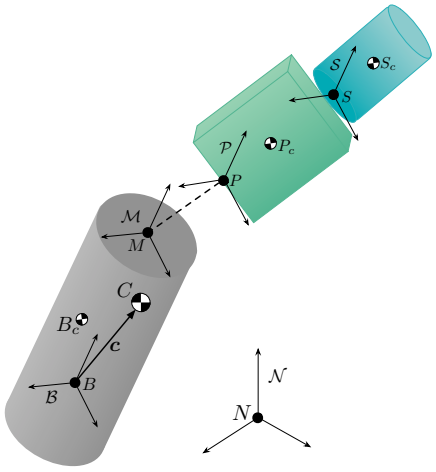

Figure 1. Problem statement for the general chained system.

Five reference frames are required to derive system dynamics. First, an inertial frame indicated

by $\mathcal{N} : \{N, \hat{\boldsymbol{n}}_1, \hat{\boldsymbol{n}}_2, \hat{\boldsymbol{n}}_3\}$ is used as the base of reference for the dynamics. The motion of the rigid hub is described using the frame $\mathcal{B} : \{B, \hat{\boldsymbol{b}}_1, \hat{\boldsymbol{b}}_2, \hat{\boldsymbol{b}}_3\}$, while the motion of the prescribed and spinning body are defined using the frames $\mathcal{P} : \{P, \hat{\boldsymbol{p}}_1, \hat{\boldsymbol{p}}_2, \hat{\boldsymbol{p}}_3\}$ and $\mathcal{S} : \{S, \hat{\boldsymbol{s}}_1, \hat{\boldsymbol{s}}_2, \hat{\boldsymbol{s}}_3\}$, respectively. The prescribed body motion is profiled relative to a hub-fixed mount frame given by $\mathcal{M} : \{M, \hat{\boldsymbol{m}}_1, \hat{\boldsymbol{m}}_2, \hat{\boldsymbol{m}}_3\}$. This frame is introduced as a matter of kinematic convenience for development of the prescribed motion. The origin points of these frames are given by N, B, M, P, and S, respectively. The masses of the system bodies are defined as m_{hub}, m_{P}, and m_{S}. Finally, the center of mass points of each body are indicated by B_c, P_c, and S_c.

The translational and rotational states required to profile the prescribed component motion are given by $\boldsymbol{r}_{P/M}, \boldsymbol{r}'_{P/M}, \boldsymbol{r}''_{P/M}, \boldsymbol{\sigma}_{\mathcal{P}/\mathcal{M}}, \boldsymbol{\omega}_{\mathcal{P}/\mathcal{M}}$ and $\boldsymbol{\omega}'_{\mathcal{P}/\mathcal{M}}$. The right $'$ superscript indicates a hub $\mathcal{B}$ frame-relative time derivative. Modified Rodriguez Parameter attitude coordinates[12] are selected to express the relative orientations between reference frames.

System Translational Equations of Motion

The spacecraft hub translational equations of motion define the first three system degrees of freedom. These equations are derived starting from Newton's Second Law for the spacecraft center of mass[12]

$$m_{\text{sc}}\ddot{\boldsymbol{r}}_{C/N} = m_{\text{sc}}\ddot{\boldsymbol{c}} + m_{\text{sc}}\ddot{\boldsymbol{r}}_{B/N} = \boldsymbol{F}_{\text{ext}} \tag{1}$$

where m_{sc} is the total mass of the spacecraft system, $m_{\text{sc}} = m_{\text{hub}} + m_{\text{P}} + m_{\text{S}}$, and $\boldsymbol{F}_{\text{ext}}$ is the sum of all external forces acting on the system. Note that because the hub equations of motion are of interest for this formulation, the acceleration of the hub frame origin point B must be defined. First, the transport theorem[12] is used to relate the hub-relative derivative of the center of mass vector to its inertial time derivative

$$\dot{\boldsymbol{c}} = \boldsymbol{c}' + \boldsymbol{\omega}_{\mathcal{B}/\mathcal{N}} \times \boldsymbol{c} \tag{2}$$

$$\ddot{\boldsymbol{c}} = \boldsymbol{c}'' + 2\boldsymbol{\omega}_{\mathcal{B}/\mathcal{N}} \times \boldsymbol{c}' + \dot{\boldsymbol{\omega}}_{\mathcal{B}/\mathcal{N}} \times \boldsymbol{c} + \boldsymbol{\omega}_{\mathcal{B}/\mathcal{N}} \times \boldsymbol{\omega}_{\mathcal{B}/\mathcal{N}} \times \boldsymbol{c} \tag{3}$$

The system center of mass vector is defined using the mass contributions from all of the system bodies

$$\boldsymbol{c} = \frac{m_{\text{hub}}\boldsymbol{r}_{B_c/B} + m_{\text{P}}\boldsymbol{r}_{P_c/B} + m_{\text{S}}\boldsymbol{r}_{S_c/B}}{m_{\text{sc}}} \tag{4}$$

The hub-relative velocity of the center of mass vector is

$$\boldsymbol{c}' = \frac{m_{\text{P}}\boldsymbol{r}'_{P_c/B} + m_{\text{S}}\boldsymbol{r}'_{S_c/B}}{m_{\text{sc}}} \tag{5}$$

where using the transport theorem yields

$$\boldsymbol{r}'_{P_c/B} = \boldsymbol{r}'_{P_c/P} + \boldsymbol{r}'_{P/M} + \boldsymbol{r}'_{M/B} = \boldsymbol{\omega}_{\mathcal{P}/\mathcal{B}} \times \boldsymbol{r}_{P_c/P} + \boldsymbol{r}'_{P/M} \tag{6}$$

$$\boldsymbol{r}'_{S_c/B} = \boldsymbol{r}'_{S_c/P} + \boldsymbol{r}'_{P/B} = \frac{^{\mathcal{P}}\text{d}}{\text{d}t}\boldsymbol{r}_{S_c/P} + \boldsymbol{\omega}_{\mathcal{P}/\mathcal{B}} \times \boldsymbol{r}_{S_c/P} + \boldsymbol{r}'_{P/B} \tag{7}$$

Similarly, the hub-relative acceleration of the center of mass vector is

$$\boldsymbol{c}'' = \frac{m_{\text{P}}\boldsymbol{r}''_{P_c/B} + m_{\text{S}}\boldsymbol{r}''_{S_c/B}}{m_{\text{sc}}} \tag{8}$$

where

$$\begin{aligned}\boldsymbol{r}''_{P_c/B} &= \boldsymbol{\omega}'_{\mathcal{P}/\mathcal{B}} \times \boldsymbol{r}_{P_c/P} + \boldsymbol{\omega}_{\mathcal{P}/\mathcal{B}} \times \boldsymbol{r}'_{P_c/P} + \boldsymbol{r}''_{P/B} \\ &= \left([\tilde{\boldsymbol{\omega}}'_{\mathcal{P}/\mathcal{B}}] + [\tilde{\boldsymbol{\omega}}_{\mathcal{P}/\mathcal{B}}]^2\right) \boldsymbol{r}_{P_c/P} + \boldsymbol{r}''_{P/B}\end{aligned} \tag{9}$$

$$\begin{aligned}\boldsymbol{r}''_{S_c/B} &= \frac{{}^{\mathcal{P}}\mathrm{d}^2}{\mathrm{d}t^2}\boldsymbol{r}_{S_c/P} + 2[\tilde{\boldsymbol{\omega}}_{\mathcal{P}/\mathcal{B}}]\frac{{}^{\mathcal{P}}\mathrm{d}}{\mathrm{d}t}\boldsymbol{r}_{S_c/P} + [\tilde{\boldsymbol{\omega}}'_{\mathcal{P}/\mathcal{B}}]\boldsymbol{r}_{S_c/P} + [\tilde{\boldsymbol{\omega}}_{\mathcal{P}/\mathcal{B}}]^2\boldsymbol{r}_{S_c/P} + \boldsymbol{r}''_{P/B} \\ &= \frac{{}^{\mathcal{P}}\mathrm{d}^2}{\mathrm{d}t^2}\boldsymbol{r}_{S_c/P} + 2[\tilde{\boldsymbol{\omega}}_{\mathcal{P}/\mathcal{B}}]\frac{{}^{\mathcal{P}}\mathrm{d}}{\mathrm{d}t}\boldsymbol{r}_{S_c/P} + \left([\tilde{\boldsymbol{\omega}}'_{\mathcal{P}/\mathcal{B}}] + [\tilde{\boldsymbol{\omega}}_{\mathcal{P}/\mathcal{B}}]^2\right) \boldsymbol{r}_{S_c/P} + \boldsymbol{r}''_{P/B}\end{aligned} \tag{10}$$

Equations 9 and 10 introduce the matrix cross-product operator, where for an arbitrary vector $\boldsymbol{v} = [v_1, v_2, v_3]^T$, the corresponding matrix cross product operator is given by $[\tilde{\boldsymbol{v}}]$

$$[\tilde{\boldsymbol{v}}] = \begin{bmatrix} 0 & -v_3 & v_2 \\ v_3 & 0 & -v_1 \\ -v_2 & v_1 & 0 \end{bmatrix} \tag{11}$$

Substituting Eqs. (3) and (8) into Eq. (1) and arranging the terms in the form of the backsubstitution method yields the system translational equations of motion

$$m_{\mathrm{sc}}\ddot{\boldsymbol{r}}_{B/N} + m_{\mathrm{sc}}[\dot{\tilde{\boldsymbol{\omega}}}_{\mathcal{B}/\mathcal{N}}]\boldsymbol{c} = \boldsymbol{F}_{\mathrm{ext}} - 2m_{\mathrm{sc}}[\tilde{\boldsymbol{\omega}}_{\mathcal{B}/\mathcal{N}}]\boldsymbol{c}' - m_{\mathrm{sc}}[\tilde{\boldsymbol{\omega}}_{\mathcal{B}/\mathcal{N}}]^2\boldsymbol{c} - m_{\mathrm{P}}\boldsymbol{r}''_{P_c/B} - m_{\mathrm{S}}\boldsymbol{r}''_{S_c/B} \tag{12}$$

Note that the equation above does not explicitly reveal the coupling between the general rigid body and the prescribed body. As written, this equation is equally valid for describing a system where both bodies are directly attached to the hub. Substituting Eq. (10) into Eq. (12) yields an expanded form that exposes the coupling terms required to simulate this specific chained system

$$\begin{aligned}&m_{\mathrm{sc}}\ddot{\boldsymbol{r}}_{B/N} + m_{\mathrm{sc}}[\dot{\tilde{\boldsymbol{\omega}}}_{\mathcal{B}/\mathcal{N}}]\boldsymbol{c} = \boldsymbol{F}_{\mathrm{ext}} - 2m_{\mathrm{sc}}[\tilde{\boldsymbol{\omega}}_{\mathcal{B}/\mathcal{N}}]\boldsymbol{c}' - m_{\mathrm{sc}}[\tilde{\boldsymbol{\omega}}_{\mathcal{B}/\mathcal{N}}]^2\boldsymbol{c} \\ &\quad \text{Prescribed and general body contributions} \left\{ -m_{\mathrm{P}}\boldsymbol{r}''_{P_c/B} - m_{\mathrm{S}}\frac{{}^{\mathcal{P}}\mathrm{d}^2}{\mathrm{d}t^2}\boldsymbol{r}_{S_c/P} \right. \\ &\quad \text{Coupling contributions} \left\{ -m_{\mathrm{S}}\left(2[\tilde{\boldsymbol{\omega}}_{\mathcal{P}/\mathcal{B}}]\frac{{}^{\mathcal{P}}\mathrm{d}}{\mathrm{d}t}\boldsymbol{r}_{S_c/P} + \left([\tilde{\boldsymbol{\omega}}'_{\mathcal{P}/\mathcal{B}}] + [\tilde{\boldsymbol{\omega}}_{\mathcal{P}/\mathcal{B}}]^2\right)\boldsymbol{r}_{S_c/P} + \boldsymbol{r}''_{P/B}\right)\right.\end{aligned} \tag{13}$$

The coupling terms required to simulate the chained system in this work are seen in the third line of Eq. (13). Indeed, if the prescribed body is removed from the system, Eq. (13) collapses and yields Eq. (12).

System Rotational Equations of Motion

The spacecraft hub rotational equations of motion describe the three remaining hub degrees of freedom. The equations are developed by separating the kinematic and kinetic differential equations. This enables convenient use of the angular velocity vector $\boldsymbol{\omega}_{\mathcal{B}/\mathcal{N}}$ in the kinetic rotational equations of motion while not limiting the choice of attitude coordinates used to describe the hub kinematic orientation. The derivation begins by applying Euler's equation to the case where the spacecraft

angular momentum is expressed about a hub-fixed point not coincident with the system center of mass:[12]

$$\dot{\boldsymbol{H}}_{\text{sc},B} = \boldsymbol{L}_B + m_{\text{sc}}\ddot{\boldsymbol{r}}_{B/N} \times \boldsymbol{c} \tag{14}$$

where $\boldsymbol{H}_{\text{sc},B}$ is the inertial angular momentum of the spacecraft system about point B and $\boldsymbol{L}_B$ is the total external torque acting on the system about point B. First, the system angular momentum about point B is

$$\begin{aligned}\boldsymbol{H}_{\text{sc},B} = \boldsymbol{H}_{\text{hub},B} + \boldsymbol{H}_{\text{P},B} + \boldsymbol{H}_{\text{S},B} = &\left([I_{\text{hub},B}] + [I_{\text{P},B}] + [I_{\text{S},B}]\right)\boldsymbol{\omega}_{\mathcal{B}/\mathcal{N}} \\ &+ [I_{\text{P},P_c}]\boldsymbol{\omega}_{\mathcal{P}/\mathcal{B}} + m_{\text{P}}[\tilde{\boldsymbol{r}}_{P_c/B}]\boldsymbol{r}'_{P_c/B} \\ &+ [I_{\text{S},S_c}]\boldsymbol{\omega}_{\mathcal{S}/\mathcal{B}} + m_{\text{S}}[\tilde{\boldsymbol{r}}_{S_c/B}]\boldsymbol{r}'_{S_c/B}\end{aligned} \tag{15}$$

where $[I_{\text{hub},B}]$, $[I_{\text{P},B}]$, and $[I_{\text{S},B}]$ are the hub, prescribed, and general body inertia tensors about point B. $[I_{\text{P},P_c}]$ and $[I_{\text{S},S_c}]$ are the prescribed and general body inertia tensors about their centers of mass. Combining all inertia tensors about point B yields the total spacecraft inertia about point B

$$[I_{\text{sc},B}] = [I_{\text{hub},B}] + [I_{\text{P},B}] + [I_{\text{S},B}] \tag{16}$$

Equation (15) becomes:

$$\begin{aligned}\boldsymbol{H}_{\text{sc},B} = &[I_{\text{sc},B}]\boldsymbol{\omega}_{\mathcal{B}/\mathcal{N}} + [I_{\text{P},P_c}]\boldsymbol{\omega}_{\mathcal{P}/\mathcal{B}} + m_{\text{P}}[\tilde{\boldsymbol{r}}_{P_c/B}]\boldsymbol{r}'_{P_c/B} \\ &+ [I_{\text{S},S_c}]\boldsymbol{\omega}_{\mathcal{S}/\mathcal{B}} + m_{\text{S}}[\tilde{\boldsymbol{r}}_{S_c/B}]\boldsymbol{r}'_{S_c/B}\end{aligned} \tag{17}$$

Next, the inertial time derivative of the total spacecraft angular momentum is expressed using the transport theorem as

$$\begin{aligned}\dot{\boldsymbol{H}}_{\text{sc},B} = &\boldsymbol{H}'_{\text{sc},B} + [\tilde{\boldsymbol{\omega}}_{\mathcal{B}/\mathcal{N}}][I_{\text{sc},B}]\boldsymbol{\omega}_{\mathcal{B}/\mathcal{N}} \\ &+ \left([\tilde{\boldsymbol{\omega}}_{\mathcal{B}/\mathcal{N}}][I_{\text{P},P_c}]\boldsymbol{\omega}_{\mathcal{P}/\mathcal{B}} + m_{\text{P}}[\tilde{\boldsymbol{\omega}}_{\mathcal{B}/\mathcal{N}}][\tilde{\boldsymbol{r}}_{P_c/B}]\boldsymbol{r}'_{P_c/B}\right) \\ &+ \left([\tilde{\boldsymbol{\omega}}_{\mathcal{B}/\mathcal{N}}][I_{\text{S},S_c}]\boldsymbol{\omega}_{\mathcal{S}/\mathcal{B}} + m_{\text{S}}[\tilde{\boldsymbol{\omega}}_{\mathcal{B}/\mathcal{N}}][\tilde{\boldsymbol{r}}_{S_c/B}]\boldsymbol{r}'_{S_c/B}\right)\end{aligned} \tag{18}$$

The $\mathcal{B}$ frame time derivative of the system angular momentum is

$$\begin{aligned}\boldsymbol{H}'_{\text{sc},B} = &[I'_{\text{sc},B}]\boldsymbol{\omega}_{\mathcal{B}/\mathcal{N}} + [I_{\text{sc},B}]\dot{\boldsymbol{\omega}}_{\mathcal{B}/\mathcal{N}} \\ &+ \left([I'_{\text{P},P_c}]\boldsymbol{\omega}_{\mathcal{P}/\mathcal{B}} + [I_{\text{P},P_c}]\boldsymbol{\omega}'_{\mathcal{P}/\mathcal{B}} + m_{\text{P}}[\tilde{\boldsymbol{r}}_{P_c/B}]\boldsymbol{r}''_{P_c/B}\right) \\ &+ \left([I'_{\text{S},S_c}]\boldsymbol{\omega}_{\mathcal{S}/\mathcal{B}} + [I_{\text{S},S_c}]\boldsymbol{\omega}'_{\mathcal{S}/\mathcal{B}} + m_{\text{S}}[\tilde{\boldsymbol{r}}_{S_c/B}]\boldsymbol{r}''_{S_c/B}\right)\end{aligned} \tag{19}$$

Using the rigid body assumption for the hub and the parallel axis theorem to express the sub-component inertias about point B yields the $\mathcal{B}$ frame derivative of the spacecraft inertia tensor

$$\begin{aligned}[I'_{\text{sc},B}] = [I'_{\text{P},B}] + [I'_{\text{S},B}] \ = &\left([I'_{\text{P},P_c}] + m_{\text{P}}\left([\tilde{\boldsymbol{r}}'_{P_c/B}][\tilde{\boldsymbol{r}}_{P_c/B}]^T + [\tilde{\boldsymbol{r}}_{P_c/B}][\tilde{\boldsymbol{r}}'_{P_c/B}]^T\right)\right) \\ &+ \left([I'_{\text{S},S_c}] + m_{\text{S}}\left([\tilde{\boldsymbol{r}}'_{S_c/B}][\tilde{\boldsymbol{r}}_{S_c/B}]^T + [\tilde{\boldsymbol{r}}_{S_c/B}][\tilde{\boldsymbol{r}}'_{S_c/B}]^T\right)\right)\end{aligned} \tag{20}$$

The inertia transport theorem[26] is used to express the sub-component inertias about their centers of mass

$$[I'_{\text{P},P_c}] = [\tilde{\boldsymbol{\omega}}_{\mathcal{P}/\mathcal{B}}][I_{\text{P},P_c}] - [I_{\text{P},P_c}][\tilde{\boldsymbol{\omega}}_{\mathcal{P}/\mathcal{B}}] \tag{21}$$

$$[I^{'}_{\mathrm{S},S_c}] = [\tilde{\boldsymbol{\omega}}_{\mathcal{S}/\mathcal{B}}][I_{\mathrm{S},S_c}] - [I_{\mathrm{S},S_c}][\tilde{\boldsymbol{\omega}}_{\mathcal{S}/\mathcal{B}}] \tag{22}$$

Equation (20) becomes

$$\begin{aligned}[I^{'}_{\mathrm{sc},B}] = &\left([\tilde{\boldsymbol{\omega}}_{\mathcal{P}/\mathcal{B}}][I_{\mathrm{P},P_c}] - [I_{\mathrm{P},P_c}][\tilde{\boldsymbol{\omega}}_{\mathcal{P}/\mathcal{B}}] + m_{\mathrm{P}}\left([\tilde{\boldsymbol{r}}^{'}_{P_c/B}][\tilde{\boldsymbol{r}}_{P_c/B}]^T + [\tilde{\boldsymbol{r}}_{P_c/B}][\tilde{\boldsymbol{r}}^{'}_{P_c/B}]^T\right)\right) \\ &+ \left([\tilde{\boldsymbol{\omega}}_{\mathcal{S}/\mathcal{B}}][I_{\mathrm{S},S_c}] - [I_{\mathrm{S},S_c}][\tilde{\boldsymbol{\omega}}_{\mathcal{S}/\mathcal{B}}] + m_{\mathrm{S}}\left([\tilde{\boldsymbol{r}}^{'}_{S_c/B}][\tilde{\boldsymbol{r}}_{S_c/B}]^T + [\tilde{\boldsymbol{r}}_{S_c/B}][\tilde{\boldsymbol{r}}^{'}_{S_c/B}]^T\right)\right)\end{aligned} \tag{23}$$

Combining these results and arranging the terms in the form of the backsubstitution method yields the system rotational equations of motion

$$\begin{aligned}m_{\mathrm{sc}}[\tilde{\boldsymbol{c}}]\ddot{\boldsymbol{r}}_{B/N} + [I_{\mathrm{sc},B}]\dot{\boldsymbol{\omega}}_{\mathcal{B}/\mathcal{N}} = \boldsymbol{L}_B &- \left([I^{'}_{\mathrm{sc},B}] + [\tilde{\boldsymbol{\omega}}_{\mathcal{B}/\mathcal{N}}][I_{\mathrm{sc},B}]\right)\boldsymbol{\omega}_{\mathcal{B}/\mathcal{N}} \\ &- \left([I^{'}_{\mathrm{P},P_c}]\boldsymbol{\omega}_{\mathcal{P}/\mathcal{B}} + [I_{\mathrm{P},P_c}]\boldsymbol{\omega}^{'}_{\mathcal{P}/\mathcal{B}} + m_{\mathrm{P}}[\tilde{\boldsymbol{r}}_{P_c/B}]\boldsymbol{r}^{''}_{P_c/B}\right) \\ &- \left([I^{'}_{\mathrm{S},S_c}]\boldsymbol{\omega}_{\mathcal{S}/\mathcal{B}} + [I_{\mathrm{S},S_c}]\boldsymbol{\omega}^{'}_{\mathcal{S}/\mathcal{B}} + m_{\mathrm{S}}[\tilde{\boldsymbol{r}}_{S_c/B}]\boldsymbol{r}^{''}_{S_c/B}\right) \\ &- \left([\tilde{\boldsymbol{\omega}}_{\mathcal{B}/\mathcal{N}}][I_{\mathrm{P},P_c}]\boldsymbol{\omega}_{\mathcal{P}/\mathcal{B}} + m_{\mathrm{P}}[\tilde{\boldsymbol{\omega}}_{\mathcal{B}/\mathcal{N}}][\tilde{\boldsymbol{r}}_{P_c/B}]\boldsymbol{r}^{'}_{P_c/B}\right) \\ &- \left([\tilde{\boldsymbol{\omega}}_{\mathcal{B}/\mathcal{N}}][I_{\mathrm{S},S_c}]\boldsymbol{\omega}_{\mathcal{S}/\mathcal{B}} + m_{\mathrm{S}}[\tilde{\boldsymbol{\omega}}_{\mathcal{B}/\mathcal{N}}][\tilde{\boldsymbol{r}}_{S_c/B}]\boldsymbol{r}^{'}_{S_c/B}\right)\end{aligned} \tag{24}$$

Similar to the translational equations of motion, note that Eq. (24) does not explicitly reveal the coupling terms associated with the chain of bodies studied in this work. The expanded translational terms are given in Eqs. (7) and (10). The following terms must also be expanded to expose the coupling terms:

$$\boldsymbol{\omega}_{\mathcal{B}/\mathcal{N}} = \boldsymbol{\omega}_{\mathcal{P}/\mathcal{N}} - \boldsymbol{\omega}_{\mathcal{P}/\mathcal{B}} \tag{25}$$

$$\boldsymbol{\omega}_{\mathcal{S}/\mathcal{B}} = \boldsymbol{\omega}_{\mathcal{S}/\mathcal{P}} + \boldsymbol{\omega}_{\mathcal{P}/\mathcal{B}} \tag{26}$$

$$\boldsymbol{\omega}^{'}_{\mathcal{S}/\mathcal{B}} = \frac{^{\mathcal{P}}\mathrm{d}}{\mathrm{d}t}\boldsymbol{\omega}_{\mathcal{S}/\mathcal{P}} + \boldsymbol{\omega}^{'}_{\mathcal{P}/\mathcal{B}} \tag{27}$$

$$[I^{'}_{\mathrm{S},S_c}] = \frac{^{\mathcal{P}}\mathrm{d}}{\mathrm{d}t}[I_{\mathrm{S},S_c}] + [\tilde{\boldsymbol{\omega}}_{\mathcal{P}/\mathcal{B}}][I_{\mathrm{S},S_c}] - [I_{\mathrm{S},S_c}][\tilde{\boldsymbol{\omega}}_{\mathcal{P}/\mathcal{B}}] \tag{28}$$

Substituting these results into the system rotational equations of motion yields the final expanded form

$$\begin{aligned}m_{\mathrm{sc}}[\tilde{\boldsymbol{c}}]\ddot{\boldsymbol{r}}_{B/N} + [I_{\mathrm{sc},B}]\dot{\boldsymbol{\omega}}_{\mathcal{B}/\mathcal{N}} = \boldsymbol{L}_B &- \left([I^{'}_{\mathrm{sc},B}] + [\tilde{\boldsymbol{\omega}}_{\mathcal{B}/\mathcal{N}}][I_{\mathrm{sc},B}]\right)\boldsymbol{\omega}_{\mathcal{B}/\mathcal{N}} \\ \text{Prescribed contributions} &\begin{cases} - \left([I^{'}_{\mathrm{P},P_c}]\boldsymbol{\omega}_{\mathcal{P}/\mathcal{B}} + [I_{\mathrm{P},P_c}]\boldsymbol{\omega}^{'}_{\mathcal{P}/\mathcal{B}} + m_{\mathrm{P}}[\tilde{\boldsymbol{r}}_{P_c/B}]\boldsymbol{r}^{''}_{P_c/B}\right) \\ - \left([\tilde{\boldsymbol{\omega}}_{\mathcal{B}/\mathcal{N}}][I_{\mathrm{P},P_c}]\boldsymbol{\omega}_{\mathcal{P}/\mathcal{B}} + m_{\mathrm{P}}[\tilde{\boldsymbol{\omega}}_{\mathcal{B}/\mathcal{N}}][\tilde{\boldsymbol{r}}_{P_c/B}]\boldsymbol{r}^{'}_{P_c/B}\right) \end{cases} \\ \text{General body contributions} &\begin{cases} - \left(\frac{^{\mathcal{P}}\mathrm{d}}{\mathrm{d}t}[I_{\mathrm{S},S_c}]\boldsymbol{\omega}_{\mathcal{S}/\mathcal{P}} + [I_{\mathrm{S},S_c}]\frac{^{\mathcal{P}}\mathrm{d}}{\mathrm{d}t}\boldsymbol{\omega}_{\mathcal{S}/\mathcal{P}} + m_{\mathrm{S}}[\tilde{\boldsymbol{r}}_{S_c/P}]\frac{^{\mathcal{P}}\mathrm{d}^2}{\mathrm{d}t^2}\boldsymbol{r}_{S_c/P}\right) \\ - \left([\tilde{\boldsymbol{\omega}}_{\mathcal{P}/\mathcal{N}}][I_{\mathrm{S},S_c}]\boldsymbol{\omega}_{\mathcal{S}/\mathcal{P}} + m_{\mathrm{S}}[\tilde{\boldsymbol{\omega}}_{\mathcal{P}/\mathcal{N}}][\tilde{\boldsymbol{r}}_{S_c/P}]\frac{^{\mathcal{P}}\mathrm{d}}{\mathrm{d}t}\boldsymbol{r}_{S_c/P}\right) \end{cases}\end{aligned}$$

$$
\text{Coupling contributions} \begin{cases}
-\dfrac{^{\mathcal{P}}\mathrm{d}}{\mathrm{d}t}[I_{\mathrm{S},S_c}]\boldsymbol{\omega}_{\mathcal{P}/\mathcal{B}} - \left([\tilde{\boldsymbol{\omega}}_{\mathcal{P}/\mathcal{B}}][I_{\mathrm{S},S_c}] - [I_{\mathrm{S},S_c}][\tilde{\boldsymbol{\omega}}_{\mathcal{P}/\mathcal{B}}]\right) \\
-[I_{\mathrm{S},S_c}]\left([\tilde{\boldsymbol{\omega}}_{\mathcal{P}/\mathcal{B}}]\boldsymbol{\omega}_{\mathcal{S}/\mathcal{P}} + \boldsymbol{\omega}'_{\mathcal{P}/\mathcal{B}}\right) + [\tilde{\boldsymbol{\omega}}_{\mathcal{P}/\mathcal{B}}][I_{\mathrm{S},S_c}]\boldsymbol{\omega}_{\mathcal{S}/\mathcal{B}} \\
-[\tilde{\boldsymbol{\omega}}_{\mathcal{P}/\mathcal{N}}][I_{\mathrm{S},S_c}]\boldsymbol{\omega}_{\mathcal{P}/\mathcal{B}} - m_{\mathrm{S}}[\tilde{\boldsymbol{r}}_{P/B}]\dfrac{^{\mathcal{P}}\mathrm{d}^2}{\mathrm{d}t^2}\boldsymbol{r}_{S_c/P} \\
-m_{\mathrm{S}}[\tilde{\boldsymbol{r}}_{S/B}]\left(2[\tilde{\boldsymbol{\omega}}_{\mathcal{P}/\mathcal{B}}]\dfrac{^{\mathcal{P}}\mathrm{d}}{\mathrm{d}t}\boldsymbol{r}_{S_c/P} + \left([\tilde{\boldsymbol{\omega}}'_{\mathcal{P}/\mathcal{B}}] + [\tilde{\boldsymbol{\omega}}_{\mathcal{P}/\mathcal{B}}]^2\right)\boldsymbol{r}_{S_c/P} + \boldsymbol{r}''_{P/B}\right) \\
-m_{\mathrm{S}}[\tilde{\boldsymbol{\omega}}_{\mathcal{P}/\mathcal{N}}][\tilde{\boldsymbol{r}}_{S_c/P}]\left([\tilde{\boldsymbol{\omega}}_{\mathcal{P}/\mathcal{B}}]\boldsymbol{r}_{S_c/P} + \boldsymbol{r}'_{P/B}\right) \\
-m_{\mathrm{S}}[\tilde{\boldsymbol{\omega}}_{\mathcal{P}/\mathcal{N}}][\tilde{\boldsymbol{r}}_{P/B}]\left(\dfrac{^{\mathcal{P}}\mathrm{d}}{\mathrm{d}t}\boldsymbol{r}_{S_c/P} + [\tilde{\boldsymbol{\omega}}_{\mathcal{P}/\mathcal{B}}]\boldsymbol{r}_{S_c/P} + \boldsymbol{r}'_{P/B}\right) \\
+m_{\mathrm{S}}[\tilde{\boldsymbol{\omega}}_{\mathcal{P}/\mathcal{B}}][\tilde{\boldsymbol{r}}_{S_c/B}]\left(\dfrac{^{\mathcal{P}}\mathrm{d}}{\mathrm{d}t}\boldsymbol{r}_{S_c/P} + [\tilde{\boldsymbol{\omega}}_{\mathcal{P}/\mathcal{B}}]\boldsymbol{r}_{S_c/P} + \boldsymbol{r}'_{P/B}\right)
\end{cases} \tag{29}
$$

The coupling terms required to simulate the chained system in this work are grouped at the end of Eq. (29). Indeed, if the prescribed body is removed from the system, Eq. (29) collapses and yields Eq. (24).

PRESCRIBED MOTION WITH ATTACHED SINGLE-AXIS ROTATING RIGID BODY DYNAMICS

This section derives the equations of motion for a three-body chained spacecraft system consisting of a rigid hub, prescribed motion component, and an attached single-axis rotating rigid body. Building upon previous work which derives the dynamics for a single-axis rotating rigid body directly attached to a rigid hub,[18] this section expands the existing derivation to include a prescribed motion actuator component.

Problem Statement

This section develops the equations of motion for the multi-body chained spacecraft system illustrated in Fig. (2). The chained system includes a rigid hub (gray), a prescribed motion component (green), and a single-axis rotating rigid body with one degrees of freedom (blue). Note that while a single chain is shown, the derivation applies for N chained connections to the rigid hub. The frame definitions and parameters are identical as described in Sec. 1. The spin axis for the rotating body is given by $\hat{\boldsymbol{s}}$.

System Translational Equations of Motion

The system translational equations of motion derivation begins from the general result given by Eq. (13) in Sec. 1. This equation is valid for any type of rigid body attached to the prescribed motion component. Using this general expression as the starting point for the single-axis spinner considered in this section, note that the general translational acceleration term relative to the prescribed component can be simplified for a single-axis rotating rigid body as

$$
\frac{^{\mathcal{P}}\mathrm{d}^2}{\mathrm{d}t^2}\boldsymbol{r}_{S_c/P} = -[\tilde{\boldsymbol{r}}_{S_c/S}]\ddot{\theta}\hat{\boldsymbol{s}} + [\tilde{\boldsymbol{\omega}}_{\mathcal{S}/\mathcal{P}}]\frac{^{\mathcal{P}}\mathrm{d}}{\mathrm{d}t}\boldsymbol{r}_{S_c/S} \tag{30}
$$

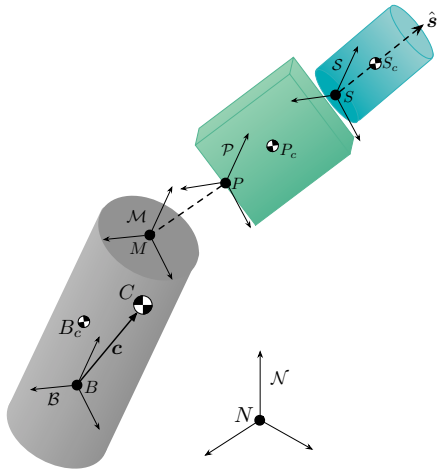

Figure 2. Problem statement for the single-axis chained system.

Substituting Eq. (30) into Eq. (13) gives the translational equations of motion for the chained system of interest in this section

$$
\begin{aligned}
&m_{\text{sc}}\ddot{\boldsymbol{r}}_{B/N} + m_{\text{sc}}[\dot{\tilde{\boldsymbol{\omega}}}_{\mathcal{B}/\mathcal{N}}]\boldsymbol{c} - m_{\text{S}}[\tilde{\boldsymbol{r}}_{S_c/S}]\ddot{\theta}\hat{\boldsymbol{s}} \\
&\qquad\qquad = \boldsymbol{F}_{\text{ext}} - 2m_{\text{sc}}[\tilde{\boldsymbol{\omega}}_{\mathcal{B}/\mathcal{N}}]\boldsymbol{c}^{'} - m_{\text{sc}}[\tilde{\boldsymbol{\omega}}_{\mathcal{B}/\mathcal{N}}]^2\boldsymbol{c} \\
&\text{Prescribed contribution}\left\{-m_{\text{P}}\boldsymbol{r}^{''}_{P_c/B}\right. \\
&\text{Spinner contribution}\left\{-m_{\text{S}}[\tilde{\boldsymbol{\omega}}_{\mathcal{S}/\mathcal{P}}]\frac{^{\mathcal{P}}\text{d}}{\text{d}t}\boldsymbol{r}_{S_c/S}\right. \\
&\text{Coupling contributions}\left\{-m_{\text{S}}\left(2[\tilde{\boldsymbol{\omega}}_{\mathcal{P}/\mathcal{B}}]\frac{^{\mathcal{P}}\text{d}}{\text{d}t}\boldsymbol{r}_{S_c/P} + \left([\tilde{\boldsymbol{\omega}}^{'}_{\mathcal{P}/\mathcal{B}}] + [\tilde{\boldsymbol{\omega}}_{\mathcal{P}/\mathcal{B}}]^2\right)\boldsymbol{r}_{S_c/P} + \boldsymbol{r}^{''}_{P/B}\right)\right.
\end{aligned}
\tag{31}
$$

Note the three groups on right-hand of Eq. (31). The first two groups indicate specific terms contributed by the prescribed and rotating bodies. The third group contains the coupling terms that result from wedging the prescribed motion component *between* the hub and spinning body. If the prescribed component is removed from the system, only the spinner contribution remains. If the spinner is removed from the system, only the prescribed contributions remain.

System Rotational Equations of Motion

Similarly, the system rotational equations of motion derivation begins from Eq. (29) derived in Sec. 1. In addition to the translational acceleration given in Eq. (30), the angular acceleration of the spinning body relative to the prescribed component must be defined

$$
\frac{^{\mathcal{P}}\text{d}}{\text{d}t}\boldsymbol{\omega}_{\mathcal{S}/\mathcal{P}} = \ddot{\theta}\hat{\boldsymbol{s}} \tag{32}
$$

Substituting the translational and rotational accelerations of the spinning body into Eq. (29) gives the rotational equations of motion for the single-axis spinner system

$$
m_{\text{sc}}[\tilde{\boldsymbol{c}}]\ddot{\boldsymbol{r}}_{B/N} + [I_{\text{sc},B}]\dot{\boldsymbol{\omega}}_{\mathcal{B}/\mathcal{N}} + \left([I_{\text{S},S_c}] - m_{\text{S}}[\tilde{\boldsymbol{r}}_{S_c/B}][\tilde{\boldsymbol{r}}_{S_c/S}]\right)\ddot{\theta}\hat{\boldsymbol{s}}
$$

$$
\begin{aligned}
&= \boldsymbol{L}_B - \left([I'_{\mathrm{sc},B}] + [\tilde{\boldsymbol{\omega}}_{\mathcal{B}/\mathcal{N}}][I_{\mathrm{sc},B}] \right) \boldsymbol{\omega}_{\mathcal{B}/\mathcal{N}} \\
\text{Prescribed contributions} \begin{cases}
&- \left([I'_{\mathrm{P},P_c}]\boldsymbol{\omega}_{\mathcal{P}/\mathcal{B}} + [I_{\mathrm{P},P_c}]\boldsymbol{\omega}'_{\mathcal{P}/\mathcal{B}} + m_{\mathrm{P}}[\tilde{\boldsymbol{r}}_{P_c/B}]\boldsymbol{r}''_{P_c/B} \right) \\
&- \left([\tilde{\boldsymbol{\omega}}_{\mathcal{B}/\mathcal{N}}][I_{\mathrm{P},P_c}]\boldsymbol{\omega}_{\mathcal{P}/\mathcal{B}} + m_{\mathrm{P}}[\tilde{\boldsymbol{\omega}}_{\mathcal{B}/\mathcal{N}}][\tilde{\boldsymbol{r}}_{P_c/B}]\boldsymbol{r}'_{P_c/B} \right)
\end{cases} \\
\text{Spinner contributions} \begin{cases}
&- \left(\dfrac{{}^{\mathcal{P}}\mathrm{d}}{\mathrm{d}t}[I_{\mathrm{S},S_c}]\boldsymbol{\omega}_{\mathcal{S}/\mathcal{P}} + m_{\mathrm{S}}[\tilde{\boldsymbol{r}}_{S_c/P}][\tilde{\boldsymbol{\omega}}_{\mathcal{S}/\mathcal{P}}]\dfrac{{}^{\mathcal{P}}\mathrm{d}}{\mathrm{d}t}\boldsymbol{r}_{S_c/S} \right) \\
&- \left([\tilde{\boldsymbol{\omega}}_{\mathcal{P}/\mathcal{N}}][I_{\mathrm{S},S_c}]\boldsymbol{\omega}_{\mathcal{S}/\mathcal{P}} + m_{\mathrm{S}}[\tilde{\boldsymbol{\omega}}_{\mathcal{P}/\mathcal{N}}][\tilde{\boldsymbol{r}}_{S_c/P}]\dfrac{{}^{\mathcal{P}}\mathrm{d}}{\mathrm{d}t}\boldsymbol{r}_{S_c/P} \right)
\end{cases} \\
\text{Coupling contributions} \begin{cases}
&- \dfrac{{}^{\mathcal{P}}\mathrm{d}}{\mathrm{d}t}[I_{\mathrm{S},S_c}]\boldsymbol{\omega}_{\mathcal{P}/\mathcal{B}} - \left([\tilde{\boldsymbol{\omega}}_{\mathcal{P}/\mathcal{B}}][I_{\mathrm{S},S_c}] - [I_{\mathrm{S},S_c}][\tilde{\boldsymbol{\omega}}_{\mathcal{P}/\mathcal{B}}] \right) \\
&- [I_{\mathrm{S},S_c}] \left([\tilde{\boldsymbol{\omega}}_{\mathcal{P}/\mathcal{B}}]\boldsymbol{\omega}_{\mathcal{S}/\mathcal{P}} + \boldsymbol{\omega}'_{\mathcal{P}/\mathcal{B}} \right) + [\tilde{\boldsymbol{\omega}}_{\mathcal{P}/\mathcal{B}}][I_{\mathrm{S},S_c}]\boldsymbol{\omega}_{\mathcal{S}/\mathcal{B}} \\
&- [\tilde{\boldsymbol{\omega}}_{\mathcal{P}/\mathcal{N}}][I_{\mathrm{S},S_c}]\boldsymbol{\omega}_{\mathcal{P}/\mathcal{B}} - m_{\mathrm{S}}[\tilde{\boldsymbol{r}}_{P/B}][\tilde{\boldsymbol{\omega}}_{\mathcal{S}/\mathcal{P}}]\dfrac{{}^{\mathcal{P}}\mathrm{d}}{\mathrm{d}t}\boldsymbol{r}_{S_c/S} \\
&- m_{\mathrm{S}}[\tilde{\boldsymbol{r}}_{S/B}] \Bigg(2[\tilde{\boldsymbol{\omega}}_{\mathcal{P}/\mathcal{B}}]\dfrac{{}^{\mathcal{P}}\mathrm{d}}{\mathrm{d}t}\boldsymbol{r}_{S_c/P} \\
&\qquad\qquad + \left([\tilde{\boldsymbol{\omega}}'_{\mathcal{P}/\mathcal{B}}] + [\tilde{\boldsymbol{\omega}}_{\mathcal{P}/\mathcal{B}}]^2 \right) \boldsymbol{r}_{S_c/P} + \boldsymbol{r}''_{P/B} \Bigg) \\
&- m_{\mathrm{S}}[\tilde{\boldsymbol{\omega}}_{\mathcal{P}/\mathcal{N}}][\tilde{\boldsymbol{r}}_{S_c/P}] \left([\tilde{\boldsymbol{\omega}}_{\mathcal{P}/\mathcal{B}}]\boldsymbol{r}_{S_c/P} + \boldsymbol{r}'_{P/B} \right) \\
&- m_{\mathrm{S}}[\tilde{\boldsymbol{\omega}}_{\mathcal{P}/\mathcal{N}}][\tilde{\boldsymbol{r}}_{P/B}] \left(\dfrac{{}^{\mathcal{P}}\mathrm{d}}{\mathrm{d}t}\boldsymbol{r}_{S_c/P} + [\tilde{\boldsymbol{\omega}}_{\mathcal{P}/\mathcal{B}}]\boldsymbol{r}_{S_c/P} + \boldsymbol{r}'_{P/B} \right) \\
&+ m_{\mathrm{S}}[\tilde{\boldsymbol{\omega}}_{\mathcal{P}/\mathcal{B}}][\tilde{\boldsymbol{r}}_{S_c/B}] \left(\dfrac{{}^{\mathcal{P}}\mathrm{d}}{\mathrm{d}t}\boldsymbol{r}_{S_c/P} + [\tilde{\boldsymbol{\omega}}_{\mathcal{P}/\mathcal{B}}]\boldsymbol{r}_{S_c/P} + \boldsymbol{r}'_{P/B} \right)
\end{cases}
\end{aligned}
\tag{33}
$$

Again note the three groups on right-hand of Eq. (33). Removing the prescribed component from the system results in all terms in these groups vanishing except the spinner contributions. Removing the spinner from the system removes all terms except the prescribed contributions.

Spinning Body Equation of Motion

Equations (31) and (33) describe the six translational and rotational degrees of freedom for the rigid hub. The equation of motion describing the final system degree of freedom is derived in Ref. [18] for the single-axis spinner attached directly to the spacecraft hub. For the chained system considered in this section, a few modifications must be made to the result. Rather than develop the equation of motion relative to the rigid hub, the spinning body equation of motion is developed relative to the prescribed component

$$
\begin{aligned}
\hat{\boldsymbol{s}}^T[I_{\mathrm{S},S}]\hat{\boldsymbol{s}}\ddot{\theta} =& u_S - m_{\mathrm{S}}\hat{\boldsymbol{s}}^T[\tilde{\boldsymbol{r}}_{S_c/S}]\ddot{\boldsymbol{r}}_{P/N} - \hat{\boldsymbol{s}}^T \left([I_{\mathrm{S},S}] - m_{\mathrm{S}}[\tilde{\boldsymbol{r}}_{S_c/S}][\tilde{\boldsymbol{r}}_{S/P}] \right) \dot{\boldsymbol{\omega}}_{\mathcal{P}/\mathcal{N}} \\
&- \hat{\boldsymbol{s}}^T[\tilde{\boldsymbol{\omega}}_{\mathcal{S}/\mathcal{N}}][I_{\mathrm{S},S}]\boldsymbol{\omega}_{\mathcal{S}/\mathcal{N}} - \hat{\boldsymbol{s}}^T[I_{\mathrm{S},S}][\tilde{\boldsymbol{\omega}}_{\mathcal{P}/\mathcal{N}}]\boldsymbol{\omega}_{\mathcal{S}/\mathcal{P}} \\
&- m_{\mathrm{S}}\hat{\boldsymbol{s}}^T[\tilde{\boldsymbol{\omega}}_{\mathcal{P}/\mathcal{N}}]\dot{\boldsymbol{r}}_{S/P}
\end{aligned}
\tag{34}
$$

Backsubstitution Formulation

Expressing the spinning body equation of motion in the form of the backsubstitution method gives the following result

$$\ddot{\theta} = \boldsymbol{a}_\theta \cdot \ddot{\boldsymbol{r}}_{P/N} + \boldsymbol{b}_\theta \cdot \dot{\boldsymbol{\omega}}_{\mathcal{P}/\mathcal{N}} + c_\theta \tag{35}$$

where

$$\boldsymbol{a}_\theta = m_{\mathrm{S}}[\tilde{\boldsymbol{r}}_{S_c/S}]\hat{\boldsymbol{s}} \;/\; \hat{\boldsymbol{s}}^T[I_{\mathrm{S},S}]\hat{\boldsymbol{s}} \tag{36a}$$

$$\boldsymbol{b}_\theta = -\left([I_{\mathrm{S},S}] - m_{\mathrm{S}}[\tilde{\boldsymbol{r}}_{S_c/S}][\tilde{\boldsymbol{r}}_{S/P}]\right)\hat{\boldsymbol{s}} \;/\; \hat{\boldsymbol{s}}^T[I_{\mathrm{S},S}]\hat{\boldsymbol{s}} \tag{36b}$$

$$\begin{aligned} c_\theta = \big(u_S - \hat{\boldsymbol{s}}^T \big([\tilde{\boldsymbol{\omega}}_{\mathcal{S}/\mathcal{N}}][I_{\mathrm{S},S}]\boldsymbol{\omega}_{\mathcal{S}/\mathcal{N}} + [I_{\mathrm{S},S}][\tilde{\boldsymbol{\omega}}_{\mathcal{P}/\mathcal{N}}]\boldsymbol{\omega}_{\mathcal{S}/\mathcal{P}}\big) \\ + m_{\mathrm{S}}[\tilde{\boldsymbol{\omega}}_{\mathcal{P}/\mathcal{N}}]\dot{\boldsymbol{r}}_{S/P}\big) \;/\; \hat{\boldsymbol{s}}^T[I_{\mathrm{S},S}]\hat{\boldsymbol{s}} \end{aligned} \tag{36c}$$

The prescribed body inertial accelerations are

$$\begin{aligned} \ddot{\boldsymbol{r}}_{P/N} &= \ddot{\boldsymbol{r}}_{P/B} + \ddot{\boldsymbol{r}}_{B/N} \\ &= \boldsymbol{r}''_{P/B} + 2[\tilde{\boldsymbol{\omega}}_{\mathcal{B}/\mathcal{N}}]\boldsymbol{r}'_{P/B} - [\tilde{\boldsymbol{r}}_{P/B}]\dot{\boldsymbol{\omega}}_{\mathcal{B}/\mathcal{N}} + [\tilde{\boldsymbol{\omega}}_{\mathcal{B}/\mathcal{N}}]^2\boldsymbol{r}_{P/B} + \ddot{\boldsymbol{r}}_{B/N} \end{aligned} \tag{37}$$

$$\dot{\boldsymbol{\omega}}_{\mathcal{P}/\mathcal{N}} = \dot{\boldsymbol{\omega}}_{\mathcal{P}/\mathcal{B}} + \dot{\boldsymbol{\omega}}_{\mathcal{B}/\mathcal{N}} = \boldsymbol{\omega}'_{\mathcal{P}/\mathcal{B}} + [\tilde{\boldsymbol{\omega}}_{\mathcal{B}/\mathcal{N}}]\boldsymbol{\omega}_{\mathcal{P}/\mathcal{B}} \tag{38}$$

Back-substituting these results into the system equations of motion given by Eqs. (31) and (33) yields the final form of the system equations of motion.

$$\begin{bmatrix} [A] & [B] \\ [C] & [D] \end{bmatrix} \begin{bmatrix} \ddot{\boldsymbol{r}}_{B/N} \\ \dot{\boldsymbol{\omega}}_{\mathcal{B}/\mathcal{N}} \end{bmatrix} = \begin{bmatrix} \boldsymbol{v}_{\text{trans}} \\ \boldsymbol{v}_{\text{rot}} \end{bmatrix} \tag{39}$$

The matrices are defined as

$$[A] = m_{\text{sc}}[I_{3\times 3}] - m_{\mathrm{S}}[\tilde{\boldsymbol{r}}_{S_c/S}]\hat{\boldsymbol{s}}\boldsymbol{a}_\theta^T \tag{40}$$

$$[B] = -m_{\text{sc}}[\tilde{\boldsymbol{c}}] - m_{\mathrm{S}}[\tilde{\boldsymbol{r}}_{S_c/S}]\hat{\boldsymbol{s}}\left(\boldsymbol{b}_\theta^T - \boldsymbol{a}_\theta^T[\tilde{\boldsymbol{r}}_{P/B}]\right) \tag{41}$$

$$[C] = m_{\text{sc}}[\tilde{\boldsymbol{c}}] + \left([I_{\mathrm{S},S_c}] - m_{\mathrm{S}}[\tilde{\boldsymbol{r}}_{S_c/B}][\tilde{\boldsymbol{r}}_{S_c/S}]\right)\hat{\boldsymbol{s}}\boldsymbol{a}_\theta^T \tag{42}$$

$$[D] = [I_{\text{sc},B}] + \left([I_{\mathrm{S},S_c}] - m_{\mathrm{S}}[\tilde{\boldsymbol{r}}_{S_c/B}][\tilde{\boldsymbol{r}}_{S_c/S}]\right)\hat{\boldsymbol{s}}\boldsymbol{b}_\theta^T \tag{43}$$

The vector components group the remaining terms

$$\begin{aligned} \boldsymbol{v}_{\text{trans}} = {} & \boldsymbol{F}_{\text{ext}} - 2m_{\text{sc}}[\tilde{\boldsymbol{\omega}}_{\mathcal{B}/\mathcal{N}}]\boldsymbol{c}' - m_{\text{sc}}[\tilde{\boldsymbol{\omega}}_{\mathcal{B}/\mathcal{N}}]^2\boldsymbol{c} \\ \text{Prescribed contributions} & \left\{ -m_{\mathrm{P}}\boldsymbol{r}''_{P_c/B} \right. \\ \text{Spinner contributions} & \left\{ -m_{\mathrm{S}}[\tilde{\boldsymbol{\omega}}_{\mathcal{S}/\mathcal{P}}]\frac{{}^{\mathcal{P}}\mathrm{d}}{\mathrm{d}t}\boldsymbol{r}_{S_c/S} + m_{\mathrm{S}}c_\theta[\tilde{\boldsymbol{r}}_{S_c/S}]\hat{\boldsymbol{s}} \right. \\ \text{Coupling contributions} & \left\{ \begin{array}{l} -m_{\mathrm{S}}\Big(2[\tilde{\boldsymbol{\omega}}_{\mathcal{P}/\mathcal{B}}]\dfrac{{}^{\mathcal{P}}\mathrm{d}}{\mathrm{d}t}\boldsymbol{r}_{S_c/P} + [\tilde{\boldsymbol{\omega}}'_{\mathcal{P}/\mathcal{B}}]\boldsymbol{r}_{S_c/P} + [\tilde{\boldsymbol{\omega}}_{\mathcal{P}/\mathcal{B}}]^2\boldsymbol{r}_{S_c/P} \\ + \boldsymbol{r}''_{P/B}\Big) + m_{\mathrm{S}}\left(\boldsymbol{a}_\theta^T\ddot{\boldsymbol{r}}_{P/B} + \boldsymbol{b}_\theta^T\dot{\boldsymbol{\omega}}_{\mathcal{P}/\mathcal{B}}\right)[\tilde{\boldsymbol{r}}_{S_c/S}]\hat{\boldsymbol{s}} \end{array} \right. \end{aligned} \tag{44}$$

$$\boldsymbol{v}_{\text{rot}} = \boldsymbol{L}_B - \left([I'_{\text{sc},B}] + [\tilde{\boldsymbol{\omega}}_{\mathcal{B}/\mathcal{N}}][I_{\text{sc},B}]\right)\boldsymbol{\omega}_{\mathcal{B}/\mathcal{N}}$$

$$
\begin{aligned}
\text{Prescribed contributions} \begin{cases} & - [I_{\mathrm{P},P_c}]\boldsymbol{\omega}'_{\mathcal{P}/\mathcal{B}} - [\tilde{\boldsymbol{\omega}}_{\mathcal{P}/\mathcal{N}}][I_{\mathrm{P},P_c}]\boldsymbol{\omega}_{\mathcal{P}/\mathcal{B}} \\ & - m_{\mathrm{P}} \left([\tilde{\boldsymbol{r}}_{P_c/B}]\boldsymbol{r}''_{P_c/B} + [\tilde{\boldsymbol{\omega}}_{\mathcal{B}/\mathcal{N}}][\tilde{\boldsymbol{r}}_{P_c/B}]\boldsymbol{r}'_{P_c/B} \right) \end{cases} \\
\text{Spinner contributions} \begin{cases} & - [\tilde{\boldsymbol{\omega}}_{\mathcal{S}/\mathcal{N}}][I_{\mathrm{S},S_c}]\boldsymbol{\omega}_{\mathcal{S}/\mathcal{P}} - m_{\mathrm{S}}[\tilde{\boldsymbol{\omega}}_{\mathcal{P}/\mathcal{N}}][\tilde{\boldsymbol{r}}_{S_c/P}]\dfrac{{}^{\mathcal{P}}\mathrm{d}}{\mathrm{d}t}\boldsymbol{r}_{S_c/P} \\ & - m_{\mathrm{S}}[\tilde{\boldsymbol{r}}_{S_c/P}][\tilde{\boldsymbol{\omega}}_{\mathcal{S}/\mathcal{P}}]\dfrac{{}^{\mathcal{P}}\mathrm{d}}{\mathrm{d}t}\boldsymbol{r}_{S_c/S} - c_\theta \left([I_{\mathrm{S},S_c}] - m_{\mathrm{S}}[\tilde{\boldsymbol{r}}_{S_c/P}][\tilde{\boldsymbol{r}}_{S_c/S}] \right) \hat{\boldsymbol{s}} \end{cases} \\
\text{Coupling contributions} \begin{cases} & - [I_{\mathrm{S},S_c}] \left([\tilde{\boldsymbol{\omega}}_{\mathcal{P}/\mathcal{B}}]\boldsymbol{\omega}_{\mathcal{S}/\mathcal{P}} + \boldsymbol{\omega}'_{\mathcal{P}/\mathcal{B}} \right) - [\tilde{\boldsymbol{\omega}}_{\mathcal{S}/\mathcal{N}}][I_{\mathrm{S},S_c}]\boldsymbol{\omega}_{\mathcal{P}/\mathcal{B}} \\ & - m_{\mathrm{S}}[\tilde{\boldsymbol{r}}_{P/B}][\tilde{\boldsymbol{\omega}}_{\mathcal{S}/\mathcal{P}}]\dfrac{{}^{\mathcal{P}}\mathrm{d}}{\mathrm{d}t}\boldsymbol{r}_{S_c/S} \\ & - m_{\mathrm{S}}[\tilde{\boldsymbol{r}}_{S_c/B}] \Bigg(2[\tilde{\boldsymbol{\omega}}_{\mathcal{P}/\mathcal{B}}]\dfrac{{}^{\mathcal{P}}\mathrm{d}}{\mathrm{d}t}\boldsymbol{r}_{S_c/P} + [\tilde{\boldsymbol{\omega}}'_{\mathcal{P}/\mathcal{B}}]\boldsymbol{r}_{S_c/P} \\ & \qquad\qquad + [\tilde{\boldsymbol{\omega}}_{\mathcal{P}/\mathcal{B}}]^2\boldsymbol{r}_{S_c/P} + \boldsymbol{r}''_{P/B} \Bigg) \\ & + m_{\mathrm{S}} \left([\tilde{\boldsymbol{\omega}}_{\mathcal{P}/\mathcal{B}}][\tilde{\boldsymbol{r}}_{S_c/B}] - [\tilde{\boldsymbol{\omega}}_{\mathcal{P}/\mathcal{N}}][\tilde{\boldsymbol{r}}_{P/B}] \right) \dfrac{{}^{\mathcal{P}}\mathrm{d}}{\mathrm{d}t}\boldsymbol{r}_{S_c/P} \\ & - m_{\mathrm{S}}[\tilde{\boldsymbol{\omega}}_{\mathcal{B}/\mathcal{N}}][\tilde{\boldsymbol{r}}_{S_c/B}] \left([\tilde{\boldsymbol{\omega}}_{\mathcal{P}/\mathcal{B}}]\boldsymbol{r}_{S_c/P} + \boldsymbol{r}'_{P/B} \right) \\ & - m_{\mathrm{S}}c_\theta[\tilde{\boldsymbol{r}}_{P/B}][\tilde{\boldsymbol{r}}_{S_c/S}]\hat{\boldsymbol{s}} \\ & - \left([I_{\mathrm{S},S_c}] - m_{\mathrm{S}}[\tilde{\boldsymbol{r}}_{S_c/B}][\tilde{\boldsymbol{r}}_{S_c/S}] \right) \hat{\boldsymbol{s}} \left(\boldsymbol{a}_\theta^T\ddot{\boldsymbol{r}}_{P/B} - \boldsymbol{b}_\theta^T\dot{\boldsymbol{\omega}}_{\mathcal{P}/\mathcal{B}} \right) \end{cases}
\end{aligned} \tag{45}
$$

Note that if the prescribed body is removed from the final results above, both the prescribed and coupling contributions vanish and the equations simplify to describe the two-body hub and spinner system derived in [18]. If the spinner is removed from the system, the equations simplify to the hub and prescribed component system derived in [19].

PRESCRIBED MOTION WITH ATTACHED DUAL-AXIS ROTATING RIGID BODY DYNAMICS

Problem Statement

The problem statement for the chained system with a dual-axis rotating rigid body is illustrated in Fig. (3). The frame definitions and parameters are identical as described in Sec. 1, with the addition of a second spinning body defined using the body frame $\mathcal{S}_2$, mass m_2 and center of mass S_{c_2}. The spin axes for the rotating bodies are given by $\hat{\boldsymbol{s}}_1$ and $\hat{\boldsymbol{s}}_2$.

System Translational Equations of Motion

The translational equations of motion for the four-body system are derived by modifying Eq. (13) for the case with two general rigid bodies attached sequentially to the prescribed motion component. Next, the translational accelerations for each spinning body relative to the prescribed body can be expressed as

$$
\frac{{}^{\mathcal{P}}\mathrm{d}^2}{\mathrm{d}t^2}\boldsymbol{r}_{S_{c_1}/P} = -[\tilde{\boldsymbol{r}}_{S_{c_1}/S_1}]\ddot{\theta}_1\hat{\boldsymbol{s}}_1 + [\tilde{\boldsymbol{\omega}}_{\mathcal{S}_1/\mathcal{P}}]\frac{{}^{\mathcal{P}}\mathrm{d}}{\mathrm{d}t}\boldsymbol{r}_{S_{c_1}/S_1} \tag{46}
$$

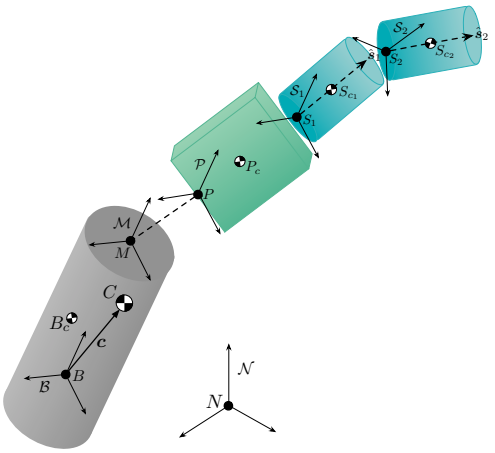

Figure 3. Problem statement for the dual-axis chained system.

$$
\begin{aligned}
\frac{^{\mathcal{P}}\mathrm{d}^2}{\mathrm{d}t^2}\boldsymbol{r}_{S_{c_2}/P} &= -[\tilde{\boldsymbol{r}}_{S_{c_2}/S_1}]\ddot{\theta}_1\hat{\boldsymbol{s}}_1 - [\tilde{\boldsymbol{r}}_{S_{c_2}/S_2}]\ddot{\theta}_2\hat{\boldsymbol{s}}_2 \\
&\quad + \left([\tilde{\boldsymbol{\omega}}_{\mathcal{S}_1/\mathcal{P}}][\tilde{\boldsymbol{\omega}}_{\mathcal{S}_2/\mathcal{S}_1}]\right)\boldsymbol{r}_{S_{c_2}/S_2} + [\tilde{\boldsymbol{\omega}}_{\mathcal{S}_2/\mathcal{S}_1}]\frac{^{\mathcal{P}}\mathrm{d}}{\mathrm{d}t}\boldsymbol{r}_{S_{c_2}/S_2} + [\tilde{\boldsymbol{\omega}}_{\mathcal{S}_1/\mathcal{P}}]\frac{^{\mathcal{P}}\mathrm{d}}{\mathrm{d}t}\boldsymbol{r}_{S_{c_2}/S_1}
\end{aligned} \tag{47}
$$

Substituting Eqs. (46) and (47) into the general system dynamics gives the dual-axis spinner system translational equations of motion

$$
\begin{aligned}
m_{\mathrm{sc}}\ddot{\boldsymbol{r}}_{B/N} + m_{\mathrm{sc}}[\tilde{\dot{\boldsymbol{\omega}}}_{\mathcal{B}/\mathcal{N}}]\boldsymbol{c} - \left(m_{\mathrm{S}_1}[\tilde{\boldsymbol{r}}_{S_{c_1}/S_1}] + m_{\mathrm{S}_2}[\tilde{\boldsymbol{r}}_{S_{c_2}/S_1}]\right)\ddot{\theta}_1\hat{\boldsymbol{s}}_1 - m_{\mathrm{S}_2}[\tilde{\boldsymbol{r}}_{S_{c_2}/S_2}]\ddot{\theta}_2\hat{\boldsymbol{s}}_2 \\
= \boldsymbol{F}_{\mathrm{ext}} - 2m_{\mathrm{sc}}[\tilde{\boldsymbol{\omega}}_{\mathcal{B}/\mathcal{N}}]\boldsymbol{c}' - m_{\mathrm{sc}}[\tilde{\boldsymbol{\omega}}_{\mathcal{B}/\mathcal{N}}]^2\boldsymbol{c}
\end{aligned}
$$

$$
\text{Prescribed and spinner contributions} \begin{cases}
-\, m_{\mathrm{P}}\boldsymbol{r}''_{P_c/B} \\
-\, m_{\mathrm{S}_1}[\tilde{\boldsymbol{\omega}}_{\mathcal{S}_1/\mathcal{P}}]\dfrac{^{\mathcal{P}}\mathrm{d}}{\mathrm{d}t}\boldsymbol{r}_{S_{c_1}/S_1} - m_{\mathrm{S}_2}[\tilde{\boldsymbol{\omega}}_{\mathcal{S}_1/\mathcal{P}}]\dfrac{^{\mathcal{P}}\mathrm{d}}{\mathrm{d}t}\boldsymbol{r}_{S_{c_2}/S_1} \\
-\, m_{\mathrm{S}_2}[\tilde{\boldsymbol{r}}_{S_{c_2}/S_2}]\left([\tilde{\boldsymbol{\omega}}_{\mathcal{S}_1/\mathcal{P}}]\boldsymbol{\omega}_{\mathcal{S}_2/\mathcal{S}_1}\right) - m_{\mathrm{S}_2}[\tilde{\boldsymbol{\omega}}_{\mathcal{S}_2/\mathcal{S}_1}]\dfrac{^{\mathcal{P}}\mathrm{d}}{\mathrm{d}t}\boldsymbol{r}_{S_{c_2}/S_2}
\end{cases}
$$

$$
\text{Coupling contributions} \begin{cases}
-\, 2[\tilde{\boldsymbol{\omega}}_{\mathcal{P}/\mathcal{B}}]\left(m_{\mathrm{S}_1}\dfrac{^{\mathcal{P}}\mathrm{d}}{\mathrm{d}t}\boldsymbol{r}_{S_{c_1}/P} + m_{\mathrm{S}_2}\dfrac{^{\mathcal{P}}\mathrm{d}}{\mathrm{d}t}\boldsymbol{r}_{S_{c_2}/P}\right) \\
-\left([\tilde{\boldsymbol{\omega}}'_{\mathcal{P}/\mathcal{B}}] + [\tilde{\boldsymbol{\omega}}_{\mathcal{P}/\mathcal{B}}]^2\right)\left(m_{\mathrm{S}_1}\boldsymbol{r}_{S_{c_1}/P} + m_{\mathrm{S}_2}\boldsymbol{r}_{S_{c_2}/P}\right) \\
+\left(m_{\mathrm{S}_1} + m_{\mathrm{S}_2}\right)\boldsymbol{r}''_{P/B}
\end{cases} \tag{48}
$$

System Rotational Equations of Motion

The angular accelerations for each spinning body are given by

$$
\frac{^{\mathcal{P}}\mathrm{d}}{\mathrm{d}t}\boldsymbol{\omega}_{\mathcal{S}_1/\mathcal{P}} = \ddot{\theta}_1\hat{\boldsymbol{s}}_1 \tag{49}
$$

$$
\frac{^{\mathcal{P}}\mathrm{d}}{\mathrm{d}t}\boldsymbol{\omega}_{\mathcal{S}_2/\mathcal{P}} = \ddot{\theta}_1\hat{\boldsymbol{s}}_1 + \ddot{\theta}_2\hat{\boldsymbol{s}}_2 + [\tilde{\boldsymbol{\omega}}_{\mathcal{S}_1/\mathcal{P}}]\boldsymbol{\omega}_{\mathcal{S}_2/\mathcal{S}_1} \tag{50}
$$

Substituting Eqs. (46), (47), (49), and (50) into Eq. (29) expanded for two general rigid bodies gives the dual-axis spinner system rotational equations of motion

$$
\begin{aligned}
&m_{\rm sc}[\tilde{\boldsymbol{c}}]\ddot{\boldsymbol{r}}_{B/N} + [I_{{\rm sc},B}]\dot{\boldsymbol{\omega}}_{\mathcal{B}/\mathcal{N}} \\
&\quad + \Big([I_{{\rm S}_1,S_{c_1}}] + [I_{{\rm S}_2,S_{c_2}}] - m_{{\rm S}_1}[\tilde{\boldsymbol{r}}_{S_{c_1}/B}][\tilde{\boldsymbol{r}}_{S_{c_1}/S_1}] - m_{{\rm S}_2}[\tilde{\boldsymbol{r}}_{S_{c_2}/B}][\tilde{\boldsymbol{r}}_{S_{c_2}/S_2}]\Big)\ddot{\theta}_1\hat{\boldsymbol{s}}_1 \\
&\quad + \Big([I_{{\rm S}_2,S_{c_2}}] - m_{{\rm S}_2}[\tilde{\boldsymbol{r}}_{S_{c_2}/B}][\tilde{\boldsymbol{r}}_{S_{c_2}/S_2}]\Big)\ddot{\theta}_2\hat{\boldsymbol{s}}_2 \\
&\quad = \boldsymbol{L}_B - \Big([I'_{{\rm sc},B}] + [\tilde{\boldsymbol{\omega}}_{\mathcal{B}/\mathcal{N}}][I_{{\rm sc},B}]\Big)\boldsymbol{\omega}_{\mathcal{B}/\mathcal{N}} \\
&\qquad \text{Prescribed contributions} \left\{ \begin{aligned}
&- \Big([I'_{{\rm P},P_c}]\boldsymbol{\omega}_{\mathcal{P}/\mathcal{B}} + [I_{{\rm P},P_c}]\boldsymbol{\omega}'_{\mathcal{P}/\mathcal{B}} + m_{\rm P}[\tilde{\boldsymbol{r}}_{P_c/B}]\boldsymbol{r}''_{P_c/B}\Big) \\
&- \Big([\tilde{\boldsymbol{\omega}}_{\mathcal{B}/\mathcal{N}}][I_{{\rm P},P_c}]\boldsymbol{\omega}_{\mathcal{P}/\mathcal{B}} + m_{\rm P}[\tilde{\boldsymbol{\omega}}_{\mathcal{B}/\mathcal{N}}][\tilde{\boldsymbol{r}}_{P_c/B}]\boldsymbol{r}'_{P_c/B}\Big)
\end{aligned} \right. \\
&\qquad \text{Dual spinner contributions} \left\{ \begin{aligned}
&- \left(\frac{^{\mathcal{P}}{\rm d}}{{\rm d}t}[I_{{\rm S}_1,S_{c_1}}]\boldsymbol{\omega}_{\mathcal{S}_1/\mathcal{P}} + m_{{\rm S}_1}[\tilde{\boldsymbol{r}}_{S_{c_1}/P}][\tilde{\boldsymbol{\omega}}_{\mathcal{S}_1/\mathcal{P}}]\frac{^{\mathcal{P}}{\rm d}}{{\rm d}t}\boldsymbol{r}_{S_{c_1}/S_1}\right) \\
&- \Big(\frac{^{\mathcal{P}}{\rm d}}{{\rm d}t}[I_{{\rm S}_2,S_{c_2}}]\boldsymbol{\omega}_{\mathcal{S}_2/\mathcal{P}} + m_{{\rm S}_2}[\tilde{\boldsymbol{r}}_{S_{c_2}/P}]\Big(\big([\tilde{\boldsymbol{\omega}}_{\mathcal{S}_1/\mathcal{P}}][\tilde{\boldsymbol{\omega}}_{\mathcal{S}_2/\mathcal{S}_1}]\big)\boldsymbol{r}_{S_{c_2}/S_2} \\
&\quad + [\tilde{\boldsymbol{\omega}}_{\mathcal{S}_2/\mathcal{S}_1}]\frac{^{\mathcal{P}}{\rm d}}{{\rm d}t}\boldsymbol{r}_{S_{c_2}/S_2} + [\tilde{\boldsymbol{\omega}}_{\mathcal{S}_1/\mathcal{P}}]\frac{^{\mathcal{P}}{\rm d}}{{\rm d}t}\boldsymbol{r}_{S_{c_2}/S_1}\Big) \\
&- \left([\tilde{\boldsymbol{\omega}}_{\mathcal{P}/\mathcal{N}}][I_{{\rm S}_1,S_{c_1}}]\boldsymbol{\omega}_{\mathcal{S}_1/\mathcal{P}} + m_{{\rm S}_1}[\tilde{\boldsymbol{\omega}}_{\mathcal{P}/\mathcal{N}}][\tilde{\boldsymbol{r}}_{S_{c_1}/P}]\frac{^{\mathcal{P}}{\rm d}}{{\rm d}t}\boldsymbol{r}_{S_{c_1}/P}\right) \\
&- \left([\tilde{\boldsymbol{\omega}}_{\mathcal{P}/\mathcal{N}}][I_{{\rm S}_2,S_{c_2}}]\boldsymbol{\omega}_{\mathcal{S}_2/\mathcal{P}} + m_{{\rm S}_2}[\tilde{\boldsymbol{\omega}}_{\mathcal{P}/\mathcal{N}}][\tilde{\boldsymbol{r}}_{S_{c_2}/P}]\frac{^{\mathcal{P}}{\rm d}}{{\rm d}t}\boldsymbol{r}_{S_{c_2}/P}\right) \\
&- [I_{{\rm S}_2,S_{c_2}}][\tilde{\boldsymbol{\omega}}_{\mathcal{S}_1/\mathcal{P}}]\boldsymbol{\omega}_{\mathcal{S}_2/\mathcal{S}_1}
\end{aligned} \right. \\
&\qquad \text{Coupling contributions} \left\{ \begin{aligned}
&- \left(\frac{^{\mathcal{P}}{\rm d}}{{\rm d}t}[I_{{\rm S}_1,S_{c_1}}] + \frac{^{\mathcal{P}}{\rm d}}{{\rm d}t}[I_{{\rm S}_2,S_{c_2}}]\right)\boldsymbol{\omega}_{\mathcal{P}/\mathcal{B}} - \big([I_{{\rm S}_1,S_{c_1}}] + [I_{{\rm S}_2,S_{c_2}}]\big)\boldsymbol{\omega}'_{\mathcal{P}/\mathcal{B}} \\
&- [\tilde{\boldsymbol{\omega}}_{\mathcal{P}/\mathcal{N}}][I_{{\rm S}_1,S_{c_1}}]\boldsymbol{\omega}_{\mathcal{P}/\mathcal{B}} - [\tilde{\boldsymbol{\omega}}_{\mathcal{P}/\mathcal{N}}][I_{{\rm S}_2,S_{c_2}}]\boldsymbol{\omega}_{\mathcal{P}/\mathcal{B}} \\
&- m_{{\rm S}_1}[\tilde{\boldsymbol{r}}_{P/B}][\tilde{\boldsymbol{\omega}}_{\mathcal{S}_1/\mathcal{P}}]\frac{^{\mathcal{P}}{\rm d}}{{\rm d}t}\boldsymbol{r}_{S_{c_1}/S_1} \\
&- m_{{\rm S}_2}[\tilde{\boldsymbol{r}}_{P/B}]\Big(\big([\tilde{\boldsymbol{\omega}}_{\mathcal{S}_1/\mathcal{P}}][\tilde{\boldsymbol{\omega}}_{\mathcal{S}_2/\mathcal{S}_1}]\big)\boldsymbol{r}_{S_{c_2}/S_2} \\
&\quad + [\tilde{\boldsymbol{\omega}}_{\mathcal{S}_2/\mathcal{S}_1}]\frac{^{\mathcal{P}}{\rm d}}{{\rm d}t}\boldsymbol{r}_{S_{c_2}/S_2} + [\tilde{\boldsymbol{\omega}}_{\mathcal{S}_1/\mathcal{P}}]\frac{^{\mathcal{P}}{\rm d}}{{\rm d}t}\boldsymbol{r}_{S_{c_2}/S_1}\Big) \\
&- m_{{\rm S}_1}[\tilde{\boldsymbol{r}}_{S_{c_1}/B}]\left(2[\tilde{\boldsymbol{\omega}}_{\mathcal{P}/\mathcal{B}}]\frac{^{\mathcal{P}}{\rm d}}{{\rm d}t}\boldsymbol{r}_{S_{c_1}/P} + \Big([\tilde{\boldsymbol{\omega}}'_{\mathcal{P}/\mathcal{B}}] + [\tilde{\boldsymbol{\omega}}_{\mathcal{P}/\mathcal{B}}]^2\Big)\boldsymbol{r}_{S_{c_1}/P} + \boldsymbol{r}''_{P/B}\right) \\
&- m_{{\rm S}_2}[\tilde{\boldsymbol{r}}_{S_{c_2}/B}]]\left(2[\tilde{\boldsymbol{\omega}}_{\mathcal{P}/\mathcal{B}}]\frac{^{\mathcal{P}}{\rm d}}{{\rm d}t}\boldsymbol{r}_{S_{c_2}/P} + \Big([\tilde{\boldsymbol{\omega}}'_{\mathcal{P}/\mathcal{B}}] + [\tilde{\boldsymbol{\omega}}_{\mathcal{P}/\mathcal{B}}]^2\Big)\boldsymbol{r}_{S_{c_2}/P} + \boldsymbol{r}''_{P/B}\right) \\
&- m_{{\rm S}_1}[\tilde{\boldsymbol{\omega}}_{\mathcal{P}/\mathcal{N}}][\tilde{\boldsymbol{r}}_{S_{c_1}/P}]\Big([\tilde{\boldsymbol{\omega}}_{\mathcal{P}/\mathcal{B}}]\boldsymbol{r}_{S_{c_1}/P} + \boldsymbol{r}'_{P/B}\Big) \\
&- m_{{\rm S}_2}[\tilde{\boldsymbol{\omega}}_{\mathcal{P}/\mathcal{N}}][\tilde{\boldsymbol{r}}_{S_{c_2}/P}]\Big([\tilde{\boldsymbol{\omega}}_{\mathcal{P}/\mathcal{B}}]\boldsymbol{r}_{S_{c_2}/P} + \boldsymbol{r}'_{P/B}\Big) \\
&- m_{{\rm S}_1}\Big([\tilde{\boldsymbol{\omega}}_{\mathcal{P}/\mathcal{N}}][\tilde{\boldsymbol{r}}_{P/B}] - [\tilde{\boldsymbol{\omega}}_{\mathcal{P}/\mathcal{B}}][\tilde{\boldsymbol{r}}_{S_{c_1}/B}]\Big)\left(\frac{^{\mathcal{P}}{\rm d}}{{\rm d}t}\boldsymbol{r}_{S_{c_1}/P} + [\tilde{\boldsymbol{\omega}}_{\mathcal{P}/\mathcal{B}}]\boldsymbol{r}_{S_{c_1}/P} + \boldsymbol{r}'_{P/B}\right) \\
&- m_{{\rm S}_2}\Big([\tilde{\boldsymbol{\omega}}_{\mathcal{P}/\mathcal{N}}][\tilde{\boldsymbol{r}}_{P/B}] - [\tilde{\boldsymbol{\omega}}_{\mathcal{P}/\mathcal{B}}][\tilde{\boldsymbol{r}}_{S_{c_2}/B}]\Big)\left(\frac{^{\mathcal{P}}{\rm d}}{{\rm d}t}\boldsymbol{r}_{S_{c_2}/P} + [\tilde{\boldsymbol{\omega}}_{\mathcal{P}/\mathcal{B}}]\boldsymbol{r}_{S_{c_2}/P} + \boldsymbol{r}'_{P/B}\right)
\end{aligned} \right.
\end{aligned}
\tag{51}
$$

First Spinning Body Equations of Motion

Equations for the two remaining degrees of freedom for the dual-axis spinner must be derived to obtain the full system dynamics. Reference [18] derives these equations of motion for the hub and dual-axis spinner system. Attaching the dual-axis spinner to the prescribed motion component yields the following modified result for the first equation of motion describing the spinning body system

$$
\begin{aligned}
&\hat{\boldsymbol{s}}_1^T[I_{\mathrm{S}_1,S_1}]\hat{\boldsymbol{s}}_1\ddot{\theta}_1 + \hat{\boldsymbol{s}}_1^T\left([I_{\mathrm{S}_2,S_{c_2}}] - m_{\mathrm{S}_2}[\tilde{\boldsymbol{r}}_{S_{c_2}/S_1}][\tilde{\boldsymbol{r}}_{S_{c_2}/S_2}]\right)\hat{\boldsymbol{s}}_2\ddot{\theta}_2 \\
&\quad = u_{S_1} - m_{\mathrm{S}}\hat{\boldsymbol{s}}_1^T[\tilde{\boldsymbol{r}}_{S_c/S_1}]\ddot{\boldsymbol{r}}_{P/N} - \hat{\boldsymbol{s}}_1^T\left([I_{\mathrm{S},S_1}] - m_{\mathrm{S}}[\tilde{\boldsymbol{r}}_{S_c/S_1}][\tilde{\boldsymbol{r}}_{S_1/P}]\right)\dot{\boldsymbol{\omega}}_{\mathcal{P}/\mathcal{N}} \\
&\qquad - \hat{\boldsymbol{s}}_1^T\left(\frac{^{\mathcal{P}}\mathrm{d}}{\mathrm{d}t}[I_{\mathrm{S},S_1}] + [\tilde{\boldsymbol{\omega}}_{\mathcal{P}/\mathcal{N}}][I_{\mathrm{S},S_1}]\right)\boldsymbol{\omega}_{\mathcal{P}/\mathcal{N}} \\
&\qquad - \hat{\boldsymbol{s}}_1^T\left(\frac{^{\mathcal{P}}\mathrm{d}}{\mathrm{d}t}[I_{\mathrm{S}_1,S_{c_1}}] + [\tilde{\boldsymbol{\omega}}_{\mathcal{P}/\mathcal{N}}][I_{\mathrm{S}_1,S_{c_1}}]\right)\boldsymbol{\omega}_{\mathcal{S}_1/\mathcal{P}} \\
&\qquad - \hat{\boldsymbol{s}}_1^T\left(\frac{^{\mathcal{P}}\mathrm{d}}{\mathrm{d}t}[I_{\mathrm{S}_2,S_{c_2}}] + [\tilde{\boldsymbol{\omega}}_{\mathcal{P}/\mathcal{N}}][I_{\mathrm{S}_2,S_{c_2}}]\right)\boldsymbol{\omega}_{\mathcal{S}_2/\mathcal{P}} \\
&\qquad - \hat{\boldsymbol{s}}_1^T\left([I_{\mathrm{S}_2,S_{c_2}}] - m_{\mathrm{S}_2}[\tilde{\boldsymbol{r}}_{S_{c_2}/S_1}][\tilde{\boldsymbol{r}}_{S_{c_2}/S_2}]\right)[\tilde{\boldsymbol{\omega}}_{\mathcal{S}_1/\mathcal{P}}]\boldsymbol{\omega}_{\mathcal{S}_2/\mathcal{S}_1} \\
&\qquad - m_{\mathrm{S}_1}\hat{\boldsymbol{s}}_1^T\left([\tilde{\boldsymbol{r}}_{S_{c_1}/S_1}][\tilde{\boldsymbol{\omega}}_{\mathcal{S}_1/\mathcal{P}}] + [\tilde{\boldsymbol{\omega}}_{\mathcal{P}/\mathcal{N}}][\tilde{\boldsymbol{r}}_{S_{c_1}/S_1}]\right)\frac{^{\mathcal{P}}\mathrm{d}}{\mathrm{d}t}\boldsymbol{r}_{S_{c_1}/S_1} \\
&\qquad - m_{\mathrm{S}_2}\hat{\boldsymbol{s}}_1^T\left([\tilde{\boldsymbol{r}}_{S_{c_2}/S_1}][\tilde{\boldsymbol{\omega}}_{\mathcal{S}_1/\mathcal{P}}] + [\tilde{\boldsymbol{\omega}}_{\mathcal{P}/\mathcal{N}}][\tilde{\boldsymbol{r}}_{S_{c_2}/S_1}]\right)\frac{^{\mathcal{P}}\mathrm{d}}{\mathrm{d}t}\boldsymbol{r}_{S_{c_2}/S_1} \\
&\qquad - m_{\mathrm{S}_2}\hat{\boldsymbol{s}}_1^T[\tilde{\boldsymbol{r}}_{S_{c_2}/S_1}][\tilde{\boldsymbol{\omega}}_{\mathcal{S}_2/\mathcal{S}_1}]\frac{^{\mathcal{P}}\mathrm{d}}{\mathrm{d}t}\boldsymbol{r}_{S_{c_2}/S_2} - m_{\mathrm{S}}\hat{\boldsymbol{s}}_1^T[\tilde{\boldsymbol{r}}_{S_c/S_1}][\tilde{\boldsymbol{\omega}}_{\mathcal{P}/\mathcal{N}}]\dot{\boldsymbol{r}}_{S_1/P}
\end{aligned}
\tag{52}
$$

Second Spinning Body Equations of Motion

Considering only the second spinning body to obtain the final system equation of motion, the results in [18] are again modified for attachment to the prescribed motion component

$$
\begin{aligned}
&\hat{\boldsymbol{s}}_2^T\left([I_{\mathrm{S}_2,S_2}] - m_{\mathrm{S}_2}[\tilde{\boldsymbol{r}}_{S_{c_2}/S_2}][\tilde{\boldsymbol{r}}_{S_2/S_1}]\right)\hat{\boldsymbol{s}}_1\ddot{\theta}_1 + \hat{\boldsymbol{s}}_2^T[I_{\mathrm{S}_2,S_2}]\hat{\boldsymbol{s}}_2\ddot{\theta}_2 \\
&\quad = u_{S_2} - m_{\mathrm{S}_2}\hat{\boldsymbol{s}}_2^T[\tilde{\boldsymbol{r}}_{S_{c_2}/S_2}]\ddot{\boldsymbol{r}}_{P/N} - \hat{\boldsymbol{s}}_2^T\left([I_{\mathrm{S}_2,S_2}] - m_{\mathrm{S}_2}[\tilde{\boldsymbol{r}}_{S_{c_2}/S_2}][\tilde{\boldsymbol{r}}_{S_2/P}]\right)\dot{\boldsymbol{\omega}}_{\mathcal{P}/\mathcal{N}} \\
&\qquad - \hat{\boldsymbol{s}}_2^T\left(\frac{^{\mathcal{P}}\mathrm{d}}{\mathrm{d}t}[I_{\mathrm{S}_2,S_2}] + [\tilde{\boldsymbol{\omega}}_{\mathcal{P}/\mathcal{N}}][I_{\mathrm{S}_2,S_2}]\right)\boldsymbol{\omega}_{\mathcal{S}_2/\mathcal{N}} \\
&\qquad - \hat{\boldsymbol{s}}_2^T[I_{\mathrm{S}_2,S_2}][\tilde{\boldsymbol{\omega}}_{\mathcal{S}_1/\mathcal{P}}]\boldsymbol{\omega}_{\mathcal{S}_2/\mathcal{S}_1} \\
&\qquad - m_{\mathrm{S}_2}\hat{\boldsymbol{s}}_2^T[\tilde{\boldsymbol{r}}_{S_{c_2}/S_2}][\tilde{\boldsymbol{\omega}}_{\mathcal{S}_1/\mathcal{N}}]\frac{^{\mathcal{P}}\mathrm{d}}{\mathrm{d}t}\boldsymbol{r}_{S_2/S_1} \\
&\qquad - m_{\mathrm{S}_2}\hat{\boldsymbol{s}}_2^T[\tilde{\boldsymbol{r}}_{S_{c_2}/S_2}][\tilde{\boldsymbol{\omega}}_{\mathcal{P}/\mathcal{N}}]\left(\dot{\boldsymbol{r}}_{S_2/S_1} + \dot{\boldsymbol{r}}_{S_1/P}\right)
\end{aligned}
\tag{53}
$$

Backsubstitution Formulation

In order to back-substitute the spinning body equations of motion into the system equations of motion, first Eqs. (52) and (53) must be arranged compactly into the matrix form

$$
[\boldsymbol{M}_\theta]\ddot{\boldsymbol{\theta}} = [\boldsymbol{A}_\theta^*]\ddot{\boldsymbol{r}}_{P/N} + [\boldsymbol{B}_\theta^*]\dot{\boldsymbol{\omega}}_{\mathcal{P}/\mathcal{N}} + [\boldsymbol{C}_\theta^*] \tag{54}
$$

where

$$[\boldsymbol{M}_\theta] = \begin{bmatrix} \hat{\boldsymbol{s}}_1^T[I_{\mathrm{S}_1,S_1}]\hat{\boldsymbol{s}}_1 & \hat{\boldsymbol{s}}_1^T\Big([I_{\mathrm{S}_2,S_{c_2}}] - m_{\mathrm{S}_2}[\tilde{\boldsymbol{r}}_{S_{c_2}/S_1}][\tilde{\boldsymbol{r}}_{S_{c_2}/S_2}]\Big)\hat{\boldsymbol{s}}_2 \\ \hat{\boldsymbol{s}}_2^T\Big([I_{\mathrm{S}_2,S_2}] - m_{\mathrm{S}_2}[\tilde{\boldsymbol{r}}_{S_{c_2}/S_2}][\tilde{\boldsymbol{r}}_{S_2/S_1}]\Big)\hat{\boldsymbol{s}}_1 & \hat{\boldsymbol{s}}_2^T[I_{\mathrm{S}_2,S_2}]\hat{\boldsymbol{s}}_2 \end{bmatrix} \tag{55}$$

$$[\boldsymbol{A}_\theta^*] = \begin{bmatrix} -m_{\mathrm{S}}\hat{\boldsymbol{s}}_1^T[\tilde{\boldsymbol{r}}_{S_c/S_1}] \\ -m_{\mathrm{S}_2}\hat{\boldsymbol{s}}_2^T[\tilde{\boldsymbol{r}}_{S_{c_2}/S_2}] \end{bmatrix} \tag{56}$$

$$[\boldsymbol{B}_\theta^*] = \begin{bmatrix} -\hat{\boldsymbol{s}}_1^T\left([I_{\mathrm{S},S_1}] - m_{\mathrm{S}}[\tilde{\boldsymbol{r}}_{S_c/S_1}][\tilde{\boldsymbol{r}}_{S_1/P}]\right) \\ -\hat{\boldsymbol{s}}_2^T\left([I_{\mathrm{S}_2,S_2}] - m_{\mathrm{S}_2}[\tilde{\boldsymbol{r}}_{S_{c_2}/S_2}][\tilde{\boldsymbol{r}}_{S_2/P}]\right) \end{bmatrix} \tag{57}$$

$$[\boldsymbol{C}_\theta^*] = \begin{bmatrix} u_{S_1} - m_{\mathrm{S}}\hat{\boldsymbol{s}}_1^T[\tilde{\boldsymbol{r}}_{S_c/S_1}]\ddot{\boldsymbol{r}}_{P/N} - \hat{\boldsymbol{s}}_1^T\left([I_{\mathrm{S},S_1}] - m_{\mathrm{S}}[\tilde{\boldsymbol{r}}_{S_c/S_1}][\tilde{\boldsymbol{r}}_{S_1/P}]\right)\dot{\boldsymbol{\omega}}_{\mathcal{P}/\mathcal{N}} \\ -\hat{\boldsymbol{s}}_1^T\left(\frac{^{\mathcal{P}}\mathrm{d}}{\mathrm{d}t}[I_{\mathrm{S},S_1}] + [\tilde{\boldsymbol{\omega}}_{\mathcal{P}/\mathcal{N}}][I_{\mathrm{S},S_1}]\right)\boldsymbol{\omega}_{\mathcal{P}/\mathcal{N}} \\ -\hat{\boldsymbol{s}}_1^T\left(\frac{^{\mathcal{P}}\mathrm{d}}{\mathrm{d}t}[I_{\mathrm{S}_1,S_{c_1}}] + [\tilde{\boldsymbol{\omega}}_{\mathcal{P}/\mathcal{N}}][I_{\mathrm{S}_1,S_{c_1}}]\right)\boldsymbol{\omega}_{\mathcal{S}_1/\mathcal{P}} \\ -\hat{\boldsymbol{s}}_1^T\left(\frac{^{\mathcal{P}}\mathrm{d}}{\mathrm{d}t}[I_{\mathrm{S}_2,S_{c_2}}] + [\tilde{\boldsymbol{\omega}}_{\mathcal{P}/\mathcal{N}}][I_{\mathrm{S}_2,S_{c_2}}]\right)\boldsymbol{\omega}_{\mathcal{S}_2/\mathcal{P}} \\ -\hat{\boldsymbol{s}}_1^T\left([I_{\mathrm{S}_2,S_{c_2}}] - m_{\mathrm{S}_2}[\tilde{\boldsymbol{r}}_{S_{c_2}/S_1}][\tilde{\boldsymbol{r}}_{S_{c_2}/S_2}]\right)[\tilde{\boldsymbol{\omega}}_{\mathcal{S}_1/\mathcal{P}}]\boldsymbol{\omega}_{\mathcal{S}_2/\mathcal{S}_1} \\ -m_{\mathrm{S}_1}\hat{\boldsymbol{s}}_1^T\left([\tilde{\boldsymbol{r}}_{S_{c_1}/S_1}][\tilde{\boldsymbol{\omega}}_{\mathcal{S}_1/\mathcal{P}}] + [\tilde{\boldsymbol{\omega}}_{\mathcal{P}/\mathcal{N}}][\tilde{\boldsymbol{r}}_{S_{c_1}/S_1}]\right)\frac{^{\mathcal{P}}\mathrm{d}}{\mathrm{d}t}\boldsymbol{r}_{S_{c_1}/S_1} \\ -m_{\mathrm{S}_2}\hat{\boldsymbol{s}}_1^T\left([\tilde{\boldsymbol{r}}_{S_{c_2}/S_1}][\tilde{\boldsymbol{\omega}}_{\mathcal{S}_1/\mathcal{P}}] + [\tilde{\boldsymbol{\omega}}_{\mathcal{P}/\mathcal{N}}][\tilde{\boldsymbol{r}}_{S_{c_2}/S_1}]\right)\frac{^{\mathcal{P}}\mathrm{d}}{\mathrm{d}t}\boldsymbol{r}_{S_{c_2}/S_1} \\ -m_{\mathrm{S}_2}\hat{\boldsymbol{s}}_1^T[\tilde{\boldsymbol{r}}_{S_{c_2}/S_1}][\tilde{\boldsymbol{\omega}}_{\mathcal{S}_2/\mathcal{S}_1}]\frac{^{\mathcal{P}}\mathrm{d}}{\mathrm{d}t}\boldsymbol{r}_{S_{c_2}/S_2} - m_{\mathrm{S}}\hat{\boldsymbol{s}}_1^T[\tilde{\boldsymbol{r}}_{S_c/S_1}][\tilde{\boldsymbol{\omega}}_{\mathcal{P}/\mathcal{N}}]\dot{\boldsymbol{r}}_{S_1/P} \\ \\ u_{S_2} - \hat{\boldsymbol{s}}_2^T\left(\frac{^{\mathcal{P}}\mathrm{d}}{\mathrm{d}t}[I_{\mathrm{S}_2,S_2}] + [\tilde{\boldsymbol{\omega}}_{\mathcal{P}/\mathcal{N}}][I_{\mathrm{S}_2,S_2}]\right)\boldsymbol{\omega}_{\mathcal{S}_2/\mathcal{N}} \\ -\hat{\boldsymbol{s}}_2^T[I_{\mathrm{S}_2,S_2}][\tilde{\boldsymbol{\omega}}_{\mathcal{S}_1/\mathcal{P}}]\boldsymbol{\omega}_{\mathcal{S}_2/\mathcal{S}_1} \\ -m_{\mathrm{S}_2}\hat{\boldsymbol{s}}_2^T[\tilde{\boldsymbol{r}}_{S_{c_2}/S_2}][\tilde{\boldsymbol{\omega}}_{\mathcal{S}_1/\mathcal{N}}]\frac{^{\mathcal{P}}\mathrm{d}}{\mathrm{d}t}\boldsymbol{r}_{S_2/S_1} \\ -m_{\mathrm{S}_2}\hat{\boldsymbol{s}}_2^T[\tilde{\boldsymbol{r}}_{S_{c_2}/S_2}][\tilde{\boldsymbol{\omega}}_{\mathcal{P}/\mathcal{N}}]\left(\dot{\boldsymbol{r}}_{S_2/S_1} + \dot{\boldsymbol{r}}_{S_1/P}\right) \end{bmatrix} \tag{58}$$

Inversion of the system mass matrix $[\boldsymbol{M}_\theta]$ isolates the spinning body accelerations on the left-hand side

$$\ddot{\boldsymbol{\theta}} = [\boldsymbol{A}_\theta]\ddot{\boldsymbol{r}}_{P/N} + [\boldsymbol{B}_\theta]\dot{\boldsymbol{\omega}}_{\mathcal{P}/\mathcal{N}} + [\boldsymbol{C}_\theta] \tag{59a}$$

$$[\boldsymbol{A}_\theta] = [\boldsymbol{M}_\theta]^{-1}[\boldsymbol{A}_\theta^*] \tag{59b}$$

$$[\boldsymbol{B}_\theta] = [\boldsymbol{M}_\theta]^{-1}[\boldsymbol{B}_\theta^*] \tag{59c}$$

$$[\boldsymbol{C}_\theta] = [\boldsymbol{M}_\theta]^{-1}[\boldsymbol{C}_\theta^*] \tag{59d}$$

Finally, back-substituting Eq. (59a) into the system equations of motion given in Eqs. (48) and (51) provides the system equations of motion in the form of the backsubstitution method given in Eq. (39). The system backsubstitution matrix components are

$$[A] = m_{\mathrm{sc}}[I_{3\times3}] - m_{\mathrm{S}}[\tilde{\boldsymbol{r}}_{S_c/S_1}]\hat{\boldsymbol{s}}_1\boldsymbol{A}_{\theta_1} - m_{\mathrm{S}_2}[\tilde{\boldsymbol{r}}_{S_{c_2}/S_2}]\hat{\boldsymbol{s}}_2\boldsymbol{A}_{\theta_2} \tag{60}$$

$$\begin{aligned}[B] = &- m_{\mathrm{sc}}[\tilde{\boldsymbol{c}}] - m_{\mathrm{S}}[\tilde{\boldsymbol{r}}_{S_c/S_1}]\hat{\boldsymbol{s}}_1\left(\boldsymbol{B}_{\theta_1} - \boldsymbol{A}_{\theta_1}[\tilde{\boldsymbol{r}}_{P/B}]\right) \\ &- m_{\mathrm{S}_2}[\tilde{\boldsymbol{r}}_{S_{c_2}/S_2}]\hat{\boldsymbol{s}}_2\left(\boldsymbol{B}_{\theta_2} - \boldsymbol{A}_{\theta_2}[\tilde{\boldsymbol{r}}_{P/B}]\right)\end{aligned} \tag{61}$$

$$
\begin{aligned}
[C] =& m_{\text{sc}}[\tilde{\boldsymbol{c}}] + \Big([I_{\text{S}_1,S_{c_1}}] + [I_{\text{S}_2,S_{c_2}}] - m_{\text{S}_1}[\tilde{\boldsymbol{r}}_{S_{c_1}/B}][\tilde{\boldsymbol{r}}_{S_{c_1}/S_1}] \\
& - m_{\text{S}_2}[\tilde{\boldsymbol{r}}_{S_{c_2}/B}][\tilde{\boldsymbol{r}}_{S_{c_2}/S_1}] \Big) \hat{\boldsymbol{s}}_1 \boldsymbol{A}_{\theta_1} \\
& + \Big([I_{\text{S}_2,S_{c_2}}] - m_{\text{S}_2}[\tilde{\boldsymbol{r}}_{S_{c_2}/B}][\tilde{\boldsymbol{r}}_{S_{c_2}/S_2}] \Big) \hat{\boldsymbol{s}}_2 \boldsymbol{A}_{\theta_2} \qquad (62) \\
[D] =& [I_{\text{sc},B}] + \Big([I_{\text{S}_1,S_{c_1}}] + [I_{\text{S}_2,S_{c_2}}] - m_{\text{S}_1}[\tilde{\boldsymbol{r}}_{S_{c_1}/B}][\tilde{\boldsymbol{r}}_{S_{c_1}/S_1}] \\
& - m_{\text{S}_2}[\tilde{\boldsymbol{r}}_{S_{c_2}/B}][\tilde{\boldsymbol{r}}_{S_{c_2}/S_1}] \Big) \hat{\boldsymbol{s}}_1 \boldsymbol{B}_{\theta_1} \\
& + \Big([I_{\text{S}_2,S_{c_2}}] - m_{\text{S}_2}[\tilde{\boldsymbol{r}}_{S_{c_2}/B}][\tilde{\boldsymbol{r}}_{S_{c_2}/S_2}] \Big) \hat{\boldsymbol{s}}_2 \boldsymbol{B}_{\theta_2} \qquad (63)
\end{aligned}
$$

The vector components are

$$
\begin{aligned}
\boldsymbol{v}_{\text{trans}} = & \boldsymbol{F}_{\text{ext}} - 2m_{\text{sc}}[\tilde{\boldsymbol{\omega}}_{\mathcal{B}/\mathcal{N}}]\boldsymbol{c}^{'} - m_{\text{sc}}[\tilde{\boldsymbol{\omega}}_{\mathcal{B}/\mathcal{N}}]^2\boldsymbol{c} \\
& \begin{array}{c}\text{Prescribed} \\ \text{contributions}\end{array} \quad \Big\{ - m_{\text{P}}\boldsymbol{r}^{''}_{P_c/B} \\
& \begin{array}{c}\text{Dual spinner} \\ \text{contributions}\end{array} \quad \begin{cases} - m_{\text{S}}[\tilde{\boldsymbol{\omega}}_{\mathcal{S}_1/\mathcal{P}}]\dfrac{^{\mathcal{P}}\text{d}}{\text{d}t}\boldsymbol{r}_{S_c/S_1} \\ - m_{\text{S}_2}\left([\tilde{\boldsymbol{\omega}}_{\mathcal{S}_2/\mathcal{S}_1}]\dfrac{^{\mathcal{P}}\text{d}}{\text{d}t}\boldsymbol{r}_{S_{c_2}/S_2} - [\tilde{\boldsymbol{r}}_{S_{c_2}/S_2}][\tilde{\boldsymbol{\omega}}_{\mathcal{S}_2/\mathcal{S}_1}]\boldsymbol{\omega}_{\mathcal{S}_2/\mathcal{S}_1} \right) \\ + m_{\text{S}}[\tilde{\boldsymbol{r}}_{S_c/S_1}]\hat{\boldsymbol{s}}_1\boldsymbol{C}_{\theta_1} + m_{\text{S}_2}[\tilde{\boldsymbol{r}}_{S_{c_2}/S_2}]\hat{\boldsymbol{s}}_2\boldsymbol{C}_{\theta_2} \end{cases} \\
& \begin{array}{c}\text{Coupling} \\ \text{contributions}\end{array} \quad \begin{cases} - 2[\tilde{\boldsymbol{\omega}}_{\mathcal{P}/\mathcal{B}}]\left(m_{\text{S}_1}\dfrac{^{\mathcal{P}}\text{d}}{\text{d}t}\boldsymbol{r}_{S_{c_1}/P} + m_{\text{S}_2}\dfrac{^{\mathcal{P}}\text{d}}{\text{d}t}\boldsymbol{r}_{S_{c_2}/P} \right) \\ - \left([\tilde{\boldsymbol{\omega}}^{'}_{\mathcal{P}/\mathcal{B}}] + [\tilde{\boldsymbol{\omega}}_{\mathcal{P}/\mathcal{B}}]^2 \right)\left(m_{\text{S}_1}\boldsymbol{r}_{S_{c_1}/P} + m_{\text{S}_2}\boldsymbol{r}_{S_{c_2}/P} \right) \\ + (m_{\text{S}_1} + m_{\text{S}_2})\,\boldsymbol{r}^{''}_{P/B} \\ + \left(m_{\text{S}_1}[\tilde{\boldsymbol{r}}_{S_{c_1}/S_1}] + m_{\text{S}_2}[\tilde{\boldsymbol{r}}_{S_{c_2}/S_2}] \right)\left(\boldsymbol{A}_{\theta_1}\ddot{\boldsymbol{r}}_{P/B} + \boldsymbol{B}_{\theta_1}\dot{\boldsymbol{\omega}}_{\mathcal{P}/\mathcal{B}} \right)\hat{\boldsymbol{s}}_1 \\ + m_{\text{S}_2}[\tilde{\boldsymbol{r}}_{S_{c_2}/S_2}]\left(\boldsymbol{A}_{\theta_2}\ddot{\boldsymbol{r}}_{P/B} + \boldsymbol{B}_{\theta_2}\dot{\boldsymbol{\omega}}_{\mathcal{P}/\mathcal{B}} \right)\hat{\boldsymbol{s}}_2 \end{cases} \qquad (64)
\end{aligned}
$$

$$
\begin{aligned}
\boldsymbol{v}_{\text{rot}} = & \boldsymbol{L}_B - \left([I^{'}_{\text{sc},B}] + [\tilde{\boldsymbol{\omega}}_{\mathcal{B}/\mathcal{N}}][I_{\text{sc},B}] \right)\boldsymbol{\omega}_{\mathcal{B}/\mathcal{N}} \\
& \begin{array}{c}\text{Prescribed} \\ \text{contributions}\end{array} \quad \begin{cases} - \left([I^{'}_{\text{P},P_c}]\boldsymbol{\omega}_{\mathcal{P}/\mathcal{B}} + [I_{\text{P},P_c}]\boldsymbol{\omega}^{'}_{\mathcal{P}/\mathcal{B}} + m_{\text{P}}[\tilde{\boldsymbol{r}}_{P_c/B}]\boldsymbol{r}^{''}_{P_c/B} \right) \\ - \left([\tilde{\boldsymbol{\omega}}_{\mathcal{B}/\mathcal{N}}][I_{\text{P},P_c}]\boldsymbol{\omega}_{\mathcal{P}/\mathcal{B}} + m_{\text{P}}[\tilde{\boldsymbol{\omega}}_{\mathcal{B}/\mathcal{N}}][\tilde{\boldsymbol{r}}_{P_c/B}]\boldsymbol{r}^{'}_{P_c/B} \right) \end{cases}
\end{aligned}
$$

$$
\begin{aligned}
&\text{Dual spinner contributions}\\
&\left\{\begin{array}{l}
-\left(\dfrac{^{\mathcal{P}}\mathrm{d}}{\mathrm{d}t}[I_{\mathrm{S}_1,S_{c_1}}]\boldsymbol{\omega}_{\mathcal{S}_1/\mathcal{P}}+m_{\mathrm{S}_1}[\tilde{\boldsymbol{r}}_{S_{c_1}/P}][\tilde{\boldsymbol{\omega}}_{\mathcal{S}_1/\mathcal{P}}]\dfrac{^{\mathcal{P}}\mathrm{d}}{\mathrm{d}t}\boldsymbol{r}_{S_{c_1}/S_1}\right)\\
-\left(\dfrac{^{\mathcal{P}}\mathrm{d}}{\mathrm{d}t}[I_{\mathrm{S}_2,S_{c_2}}]\boldsymbol{\omega}_{\mathcal{S}_2/\mathcal{P}}+m_{\mathrm{S}_2}[\tilde{\boldsymbol{r}}_{S_{c_2}/P}]\left(\left([\tilde{\boldsymbol{\omega}}_{\mathcal{S}_1/\mathcal{P}}][\tilde{\boldsymbol{\omega}}_{\mathcal{S}_2/\mathcal{S}_1}]\right)\boldsymbol{r}_{S_{c_2}/S_2}\right.\right.\\
\quad\left.\left.+\,[\tilde{\boldsymbol{\omega}}_{\mathcal{S}_2/\mathcal{S}_1}]\dfrac{^{\mathcal{P}}\mathrm{d}}{\mathrm{d}t}\boldsymbol{r}_{S_{c_2}/S_2}+[\tilde{\boldsymbol{\omega}}_{\mathcal{S}_1/\mathcal{P}}]\dfrac{^{\mathcal{P}}\mathrm{d}}{\mathrm{d}t}\boldsymbol{r}_{S_{c_2}/S_1}\right)\right.\\
-\left([\tilde{\boldsymbol{\omega}}_{\mathcal{P}/\mathcal{N}}][I_{\mathrm{S}_1,S_{c_1}}]\boldsymbol{\omega}_{\mathcal{S}_1/\mathcal{P}}+m_{\mathrm{S}_1}[\tilde{\boldsymbol{\omega}}_{\mathcal{P}/\mathcal{N}}][\tilde{\boldsymbol{r}}_{S_{c_1}/P}]\dfrac{^{\mathcal{P}}\mathrm{d}}{\mathrm{d}t}\boldsymbol{r}_{S_{c_1}/P}\right)\\
-\left([\tilde{\boldsymbol{\omega}}_{\mathcal{P}/\mathcal{N}}][I_{\mathrm{S}_2,S_{c_2}}]\boldsymbol{\omega}_{\mathcal{S}_2/\mathcal{P}}+m_{\mathrm{S}_2}[\tilde{\boldsymbol{\omega}}_{\mathcal{P}/\mathcal{N}}][\tilde{\boldsymbol{r}}_{S_{c_2}/P}]\dfrac{^{\mathcal{P}}\mathrm{d}}{\mathrm{d}t}\boldsymbol{r}_{S_{c_2}/P}\right)\\
-[I_{\mathrm{S}_2,S_{c_2}}][\tilde{\boldsymbol{\omega}}_{\mathcal{S}_1/\mathcal{P}}]\boldsymbol{\omega}_{\mathcal{S}_2/\mathcal{S}_1}\\
-\left([I_{\mathrm{S}_1,S_{c_1}}]+[I_{\mathrm{S}_2,S_{c_2}}]-m_{\mathrm{S}_1}[\tilde{\boldsymbol{r}}_{S_{c_1}/P}][\tilde{\boldsymbol{r}}_{S_{c_1}/S_1}]-m_{\mathrm{S}_2}[\tilde{\boldsymbol{r}}_{S_{c_2}/P}][\tilde{\boldsymbol{r}}_{S_{c_2}/S_1}]\right)\boldsymbol{C}_{\theta_1}\hat{\boldsymbol{s}}_1\\
-\left([I_{\mathrm{S}_2,S_{c_2}}]-m_{\mathrm{S}_2}[\tilde{\boldsymbol{r}}_{S_{c_2}/P}][\tilde{\boldsymbol{r}}_{S_{c_2}/S_2}]\right)\boldsymbol{C}_{\theta_2}\hat{\boldsymbol{s}}_2
\end{array}\right.\\
&\text{Coupling contributions}\\
&\left\{\begin{array}{l}
-\left(\dfrac{^{\mathcal{P}}\mathrm{d}}{\mathrm{d}t}[I_{\mathrm{S}_1,S_{c_1}}]+\dfrac{^{\mathcal{P}}\mathrm{d}}{\mathrm{d}t}[I_{\mathrm{S}_2,S_{c_2}}]\right)\boldsymbol{\omega}_{\mathcal{P}/\mathcal{B}}-\left([I_{\mathrm{S}_1,S_{c_1}}]+[I_{\mathrm{S}_2,S_{c_2}}]\right)\boldsymbol{\omega}'_{\mathcal{P}/\mathcal{B}}\\
-[\tilde{\boldsymbol{\omega}}_{\mathcal{P}/\mathcal{N}}][I_{\mathrm{S}_1,S_{c_1}}]\boldsymbol{\omega}_{\mathcal{P}/\mathcal{B}}-[\tilde{\boldsymbol{\omega}}_{\mathcal{P}/\mathcal{N}}][I_{\mathrm{S}_2,S_{c_2}}]\boldsymbol{\omega}_{\mathcal{P}/\mathcal{B}}\\
-m_{\mathrm{S}_1}[\tilde{\boldsymbol{r}}_{P/B}][\tilde{\boldsymbol{\omega}}_{\mathcal{S}_1/\mathcal{P}}]\dfrac{^{\mathcal{P}}\mathrm{d}}{\mathrm{d}t}\boldsymbol{r}_{S_{c_1}/S_1}\\
-m_{\mathrm{S}_2}[\tilde{\boldsymbol{r}}_{P/B}]\left(\left([\tilde{\boldsymbol{\omega}}_{\mathcal{S}_1/\mathcal{P}}][\tilde{\boldsymbol{\omega}}_{\mathcal{S}_2/\mathcal{S}_1}]\right)\boldsymbol{r}_{S_{c_2}/S_2}\right.\\
\quad\left.+\,[\tilde{\boldsymbol{\omega}}_{\mathcal{S}_2/\mathcal{S}_1}]\dfrac{^{\mathcal{P}}\mathrm{d}}{\mathrm{d}t}\boldsymbol{r}_{S_{c_2}/S_2}+[\tilde{\boldsymbol{\omega}}_{\mathcal{S}_1/\mathcal{P}}]\dfrac{^{\mathcal{P}}\mathrm{d}}{\mathrm{d}t}\boldsymbol{r}_{S_{c_2}/S_1}\right)\\
-m_{\mathrm{S}_1}[\tilde{\boldsymbol{r}}_{S_{c_1}/B}]\left(2[\tilde{\boldsymbol{\omega}}_{\mathcal{P}/\mathcal{B}}]\dfrac{^{\mathcal{P}}\mathrm{d}}{\mathrm{d}t}\boldsymbol{r}_{S_{c_1}/P}+\left([\tilde{\boldsymbol{\omega}}'_{\mathcal{P}/\mathcal{B}}]+[\tilde{\boldsymbol{\omega}}_{\mathcal{P}/\mathcal{B}}]^2\right)\boldsymbol{r}_{S_{c_1}/P}+\boldsymbol{r}''_{P/B}\right)\\
-m_{\mathrm{S}_2}[\tilde{\boldsymbol{r}}_{S_{c_2}/B}]]\left(2[\tilde{\boldsymbol{\omega}}_{\mathcal{P}/\mathcal{B}}]\dfrac{^{\mathcal{P}}\mathrm{d}}{\mathrm{d}t}\boldsymbol{r}_{S_{c_2}/P}+\left([\tilde{\boldsymbol{\omega}}'_{\mathcal{P}/\mathcal{B}}]+[\tilde{\boldsymbol{\omega}}_{\mathcal{P}/\mathcal{B}}]^2\right)\boldsymbol{r}_{S_{c_2}/P}+\boldsymbol{r}''_{P/B}\right)\\
-m_{\mathrm{S}_1}[\tilde{\boldsymbol{\omega}}_{\mathcal{P}/\mathcal{N}}][\tilde{\boldsymbol{r}}_{S_{c_1}/P}]\left([\tilde{\boldsymbol{\omega}}_{\mathcal{P}/\mathcal{B}}]\boldsymbol{r}_{S_{c_1}/P}+\boldsymbol{r}'_{P/B}\right)\\
-m_{\mathrm{S}_2}[\tilde{\boldsymbol{\omega}}_{\mathcal{P}/\mathcal{N}}][\tilde{\boldsymbol{r}}_{S_{c_2}/P}]\left([\tilde{\boldsymbol{\omega}}_{\mathcal{P}/\mathcal{B}}]\boldsymbol{r}_{S_{c_2}/P}+\boldsymbol{r}'_{P/B}\right)\\
-m_{\mathrm{S}_1}\left([\tilde{\boldsymbol{\omega}}_{\mathcal{P}/\mathcal{N}}][\tilde{\boldsymbol{r}}_{P/B}]-[\tilde{\boldsymbol{\omega}}_{\mathcal{P}/\mathcal{B}}][\tilde{\boldsymbol{r}}_{S_{c_1}/B}]\right)\left(\dfrac{^{\mathcal{P}}\mathrm{d}}{\mathrm{d}t}\boldsymbol{r}_{S_{c_1}/P}+[\tilde{\boldsymbol{\omega}}_{\mathcal{P}/\mathcal{B}}]\boldsymbol{r}_{S_{c_1}/P}+\boldsymbol{r}'_{P/B}\right)\\
-m_{\mathrm{S}_2}\left([\tilde{\boldsymbol{\omega}}_{\mathcal{P}/\mathcal{N}}][\tilde{\boldsymbol{r}}_{P/B}]-[\tilde{\boldsymbol{\omega}}_{\mathcal{P}/\mathcal{B}}][\tilde{\boldsymbol{r}}_{S_{c_2}/B}]\right)\left(\dfrac{^{\mathcal{P}}\mathrm{d}}{\mathrm{d}t}\boldsymbol{r}_{S_{c_2}/P}+[\tilde{\boldsymbol{\omega}}_{\mathcal{P}/\mathcal{B}}]\boldsymbol{r}_{S_{c_2}/P}+\boldsymbol{r}'_{P/B}\right)\\
-\left([I_{\mathrm{S}_1,S_{c_1}}]+[I_{\mathrm{S}_2,S_{c_2}}]-m_{\mathrm{S}_1}[\tilde{\boldsymbol{r}}_{S_{c_1}/B}][\tilde{\boldsymbol{r}}_{S_{c_1}/S_1}]\right.\\
\quad\left.-m_{\mathrm{S}_2}[\tilde{\boldsymbol{r}}_{S_{c_2}/B}][\tilde{\boldsymbol{r}}_{S_{c_2}/S_1}]\right)\left(\boldsymbol{A}_{\theta_1}\ddot{\boldsymbol{r}}_{P/B}+\boldsymbol{B}_{\theta_1}\dot{\boldsymbol{\omega}}_{\mathcal{P}/\mathcal{B}}\right)\hat{\boldsymbol{s}}_1\\
-\left([I_{\mathrm{S}_2,S_{c_2}}]-m_{\mathrm{S}_2}[\tilde{\boldsymbol{r}}_{S_{c_2}/B}][\tilde{\boldsymbol{r}}_{S_{c_2}/S_2}]\right)\left(\boldsymbol{A}_{\theta_2}\ddot{\boldsymbol{r}}_{P/B}+\boldsymbol{B}_{\theta_2}\dot{\boldsymbol{\omega}}_{\mathcal{P}/\mathcal{B}}\right)\hat{\boldsymbol{s}}_2\\
+\left(m_{\mathrm{S}_1}[\tilde{\boldsymbol{r}}_{P/B}][\tilde{\boldsymbol{r}}_{S_{c_1}/S_1}]+m_{\mathrm{S}_2}[\tilde{\boldsymbol{r}}_{P/B}][\tilde{\boldsymbol{r}}_{S_{c_2}/S_1}]\right)\boldsymbol{C}_{\theta_1}\hat{\boldsymbol{s}}_1\\
+m_{\mathrm{S}_2}[\tilde{\boldsymbol{r}}_{P/B}][\tilde{\boldsymbol{r}}_{S_{c_2}/S_2}]\boldsymbol{C}_{\theta_2}\hat{\boldsymbol{s}}_2
\end{array}\right.
\end{aligned}
\tag{65}
$$

As previously mentioned, if the prescribed body is removed from the final results above the equations simplify to describe the hub and dual-spinner system derived in [18].

Table 3. Rigid hub simulation parameters.

Parameter	Notation	Value	Unit
Hub mass	m_{hub}	15,000	kg
Hub length	l_{hub}	8	m
Hub width	w_{hub}	8	m
Hub depth (height)	d_{hub}	20	m
Hub inertia about its center of mas	${}^{\mathcal{B}}[I_{\text{hub},B_c}]$	$\begin{bmatrix} 580,000 & 0 & 0 \\ 0 & 160,000 & 0 \\ 0 & 0 & 580,000 \end{bmatrix}$	kg $\cdot$ m^2
Hub center of mass location with respect to point B	${}^{\mathcal{B}}\boldsymbol{r}_{B_c/B}$	[0, 0, 0]	m
Hub initial inertial angular velocity	${}^{\mathcal{B}}\boldsymbol{\omega}_{\mathcal{B}/\mathcal{N}}$	[0.001, -0.001, 0.001]	rad / s

NUMERICAL SIMULATION

This section demonstrates the applicability of the dynamics derived in this work through a multi-body spacecraft simulation scenario. The derived dynamics for the single-axis and dual-axis spinner chained systems are implemented in the open-source Basilisk astrodynamics simulation software. The dual-axis chained system is chosen for simulation in this work.

The spacecraft simulation geometry is illustrated in Fig. (4). The spacecraft consists of a rigid hub (gray), two prescribed trusses (green) which rotate about their longitudinal axes, and eight dual-axis solar panels (blue) which rotate about their longitudinal and transverse axes. Tables (3-5) provide the spacecraft hub, prescribed truss, and spinner mass and geometric parameters selected for the simulation, respectively.

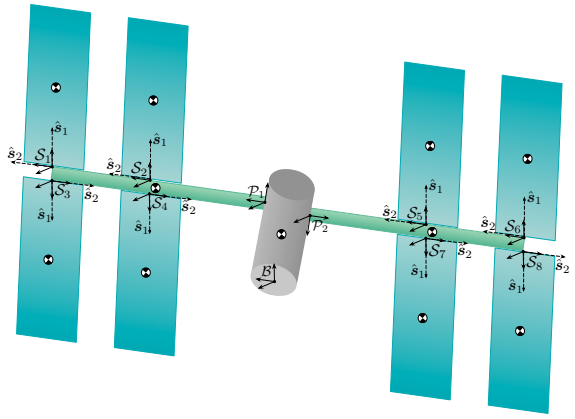

Figure 4. Spacecraft simulation setup.

The simulation sets up the spacecraft system with dispersed initial deflections for each of the solar panels about their longitudinal spin axes. At the start of the simulation, the solar panels are simultaneously released from their deflected positions while the prescribed trusses begin articulating

Table 4. Prescribed truss parameters.

Parameter	Notation	Value	Unit
Truss mass	m_{P}	6000	kg
Truss length	l_{P}	50	m
Truss width	w_{P}	4	m
Truss depth (height)	d_{P}	4	m
Truss inertia about its center of mass	${}^{\mathcal{P}}[I_{\mathrm{P},P_c}]$	$\begin{bmatrix} 1,258,000 & 0 & 0 \\ 0 & 1,258,000 & 0 \\ 0 & 0 & 16,000 \end{bmatrix}$	$\mathrm{kg} \cdot \mathrm{m}^2$
Truss center of mass locations with respect to points P	${}^{\mathcal{P}}\boldsymbol{r}_{P_c/P}$	[25, 0, 0]	m
Truss 1 mount frame location with respect to point B	${}^{\mathcal{B}}\boldsymbol{r}_{M_1/B}$	[4, 0, 0]	m
Truss 2 mount frame location with respect to point B	${}^{\mathcal{B}}\boldsymbol{r}_{M_2/B}$	[-4, 0, 0]	m
DCM of mount frame 1 with respect to the $\mathcal{B}$ frame	$[\mathcal{M}_1\mathcal{B}]$	$\begin{bmatrix} 1 & 0 & 0 \\ 0 & 1 & 0 \\ 0 & 0 & 1 \end{bmatrix}$	—
DCM of mount frame 2 with respect to the $\mathcal{B}$ frame	$[\mathcal{M}_2\mathcal{B}]$	$\begin{bmatrix} -1 & 0 & 0 \\ 0 & 1 & 0 \\ 0 & 0 & -1 \end{bmatrix}$	—
Truss rotation axes	${}^{\mathcal{M}}\hat{\boldsymbol{p}}_\theta$	[1, 0, 0]	—

Table 5. Dual-axis solar panel parameters (selected).

Parameter	Notation	Value	Unit
Panel mass	m_{S}	1000	kg
Panel length	l_{S}	10	m
Panel width	w_{S}	0.3	m
Panel depth (height)	d_{S}	30	m
Panel inertia about its center of mass	${}^{\mathcal{S}}[I_{\mathrm{S},S_c}]$	$\begin{bmatrix} 83,333.333 & 0 & 0 \\ 0 & 8,340.833 & 0 \\ 0 & 0 & 76,333.333 \end{bmatrix}$	kg $\cdot$ m^2
Panel center of mass locations with respect to points S	${}^{\mathcal{S}}\boldsymbol{r}_{S_c/S}$	[0, 0, 15]	m
Panel torsional rotation axes	${}^{\mathcal{S}}\hat{\boldsymbol{s}}_1$	[0, 0, 1]	—
Panel bending rotation axes	${}^{\mathcal{S}}\hat{\boldsymbol{s}}_2$	[1, 0, 0]	—
Torsional linear spring constant for $\hat{\boldsymbol{s}}_1$	k_1	20,000	N $\cdot$ m / rad
Torsional linear spring constant for $\hat{\boldsymbol{s}}_2$	k_2	20,000	N $\cdot$ m / rad
Torsional linear damper constant for $\hat{\boldsymbol{s}}_1$	c_1	15,000	N $\cdot$ m / rad
Torsional linear damper constant for $\hat{\boldsymbol{s}}_2$	c_2	15,000	N $\cdot$ m / rad

to achieve a 10 degree displacement about their longitudinal axes. The truss angles throughout the duration of the simulation are given in Fig. (5). The solar panel torsional and bending angles throughout the simulation are shown in Fig. 6(a) and 6(b).

Note that the solar panel bending angles are set to zero at the start of the simulation. Viewing Fig. 6(b), it is clear that these angles fluctuate throughout the simulation and displace opposite to the accelerations imparted to the spacecraft system by the prescribed truss actuation. At the start of the simulation, the truss accelerations cause the initial bending displacements. The final decelerations as the truss' complete their actuation cause the second set of visible bending displacements which are opposite to the first acceleration response. After the trusses complete their actuation, the solar panel bending angles begin damped oscillations returning towards zero.

The hub response throughout the simulation is provided in Figs. 6(c) and 6(d). As expected, the hub is seen to naturally slew about the first inertial axis in response to the rotational motion of the trusses in order to conserve the spacecraft angular momentum.

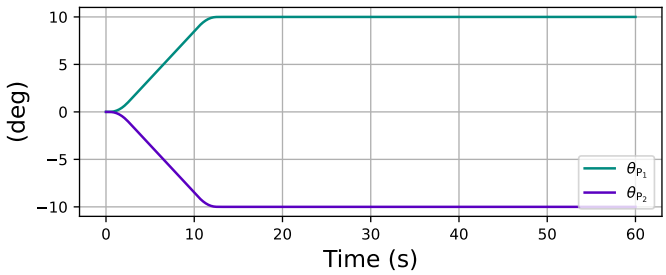

Figure 5. Prescribed truss angles.

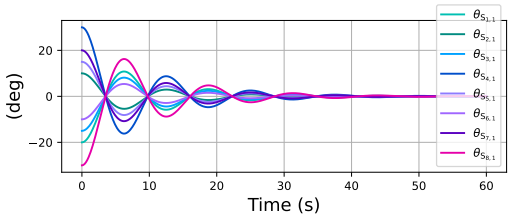

(a) Panel torsional angles (θ_1 about $\hat{\boldsymbol{s}}_1$).

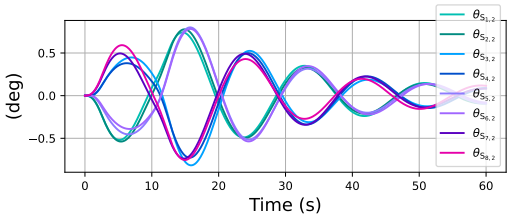

(b) Panel bending angles (θ_2 about $\hat{\boldsymbol{s}}_2$).

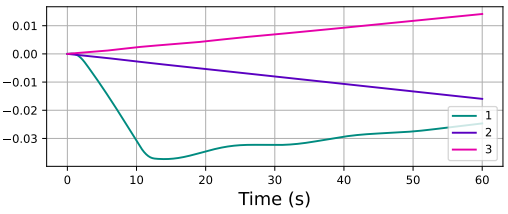

(c) Hub attitude $\boldsymbol{\sigma}_{\mathcal{B}/\mathcal{N}}$.

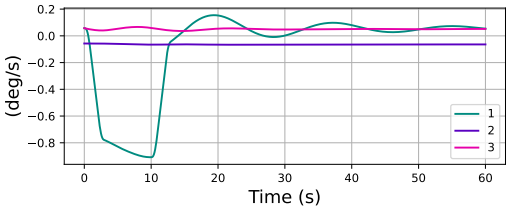

(d) Hub angular velocity $\boldsymbol{\omega}_{\mathcal{B}/\mathcal{N}}$.

Figure 6. Simulation scenario results.

CONCLUSION

Advancements in spacecraft structures and their attached appendages such as robotic arms and gimballed platforms require extensive simulation developments in order to verify mission requirements and confirm the reliability of new spacecraft concepts. This work expands the current spacecraft simulation space under the assumptions of the backsubstitution method by integrating kinematically prescribed spacecraft components with single- and dual-axis rotating components and developing the equations of motion for these chained systems.

First, the general dynamics for a three-body chained system consisting of a rigid hub, kinematically prescribed component, and a general rigid body are derived. The results are used as the derivation starting point for the chained system containing the single-axis spinner. The derivation can be easily expanded for N branches relative to the spacecraft hub. A second derivation outlines the procedure for a dual-axis rotating rigid body attached to the prescribed component rather than the single-axis spinner. The results are used to attach four dual-axis solar panels to each of two prescribed motion trusses in a spacecraft simulation scenario, illustrating the applicability of this

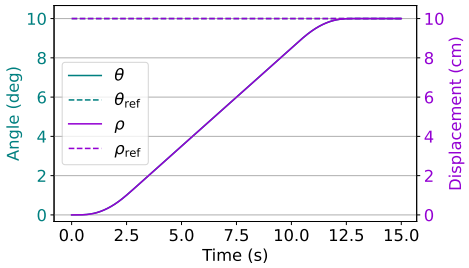

(a) Prescribed angle $\theta(t)$ and displacement $\rho(t)$.

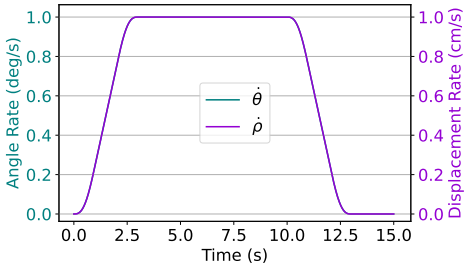

(b) Prescribed rates $\dot{\theta}(t)$ and $\dot{\rho}(t)$.

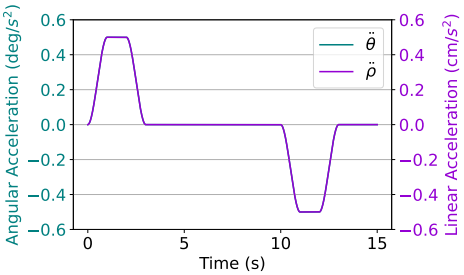

(c) Prescribed accelerations $\ddot{\theta}(t)$ and $\ddot{\rho}(t)$.

Figure 7. Prescribed states for both verification scenarios.

work. The hub response to initial deflections of all eight panels is studied while both prescribed trusses articulate to specified reference angles. The appendix verifies the derived dynamics for both spinner systems by checking that the quantities of orbital energy, orbital angular momentum, and spacecraft angular momentum remain constant in a conservative environment.

APPENDIX: DYNAMICS VERIFICATION

In order to draw meaningful conclusions from numerical simulations, it is important to use a verification approach to ensure the system dynamics are correctly derived and implemented in software. The derived equations of motion for the systems studied in this work are verified by checking that the quantities of orbital angular momentum, orbital energy, and the spacecraft rotational angular momentum remain constant in a conservative environment.[14] The spacecraft rotational energy is not checked because the accelerations and decelerations imparted onto the system by the prescribed body add and remove energy from the system, respectively. Instead, this quantity is checked to return zero at the end of the simulation.

A rigid hub with a single connected prescribed sub-component is simulated for both verification scenarios. The first scenario checks conservation for the single-axis spinner system, while the second checks conservation for the dual-axis spinner system. The profiled hub-relative motion for the prescribed motion body is shown in Fig. (7). The prescribed body simultaneously translates and rotates throughout the scenario, displacing 10 centimeters and rotating

Prescribed Motion with Attached Single-Axis Rotating Rigid Body

Verification of the single-axis spinner system are given in Fig. (8).

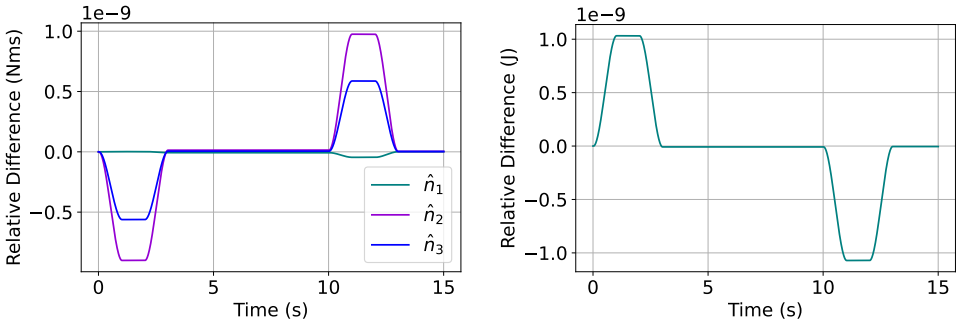

(a) Orbital angular momentum.

(b) Orbital energy.

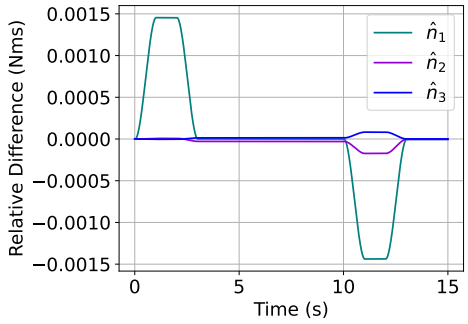

(c) Rotational angular momentum.

Figure 8. Verification results for the single-axis spinner system.

Prescribed Motion with Attached Dual-Axis Rotating Rigid Body

Verification of the dual-axis spinner system are given in Fig. (9).

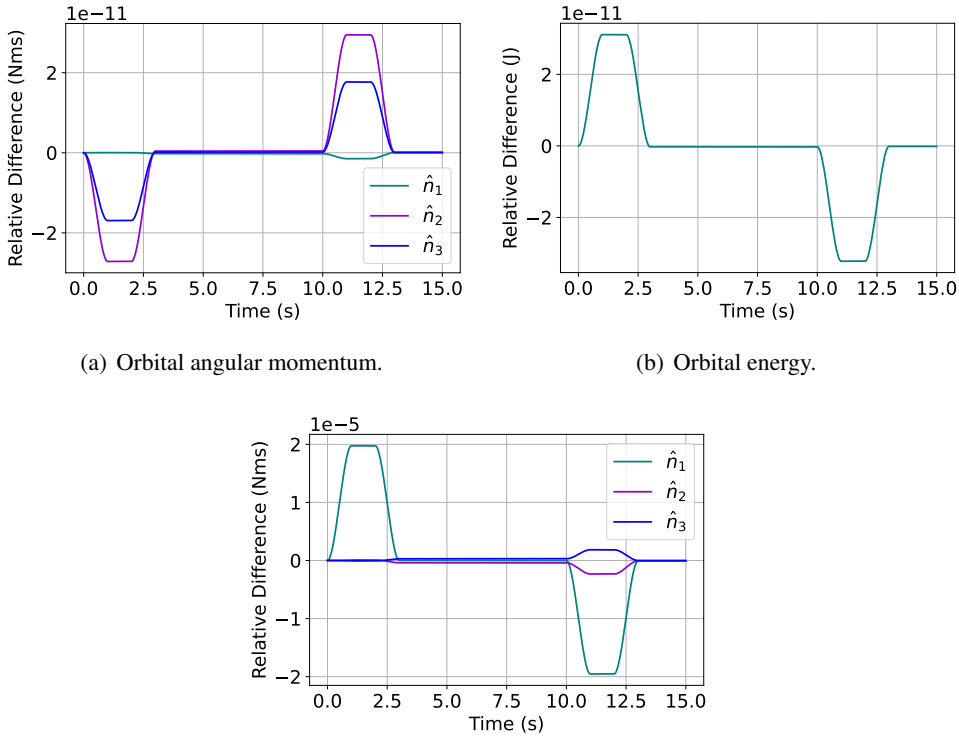

(a) Orbital angular momentum.

(b) Orbital energy.

(c) Rotational angular momentum.

Figure 9. Verification results for the dual-axis spinner system.

REFERENCES

[1] A. K. Banerjee, "Contributions of Multibody Dynamics to Space Flight: A Brief Review," *Journal of Guidance, Control, and Dynamics*, Vol. 26, No. 3, 2003, pp. 385–394.

[2] J. Gibb, "Lightweight Flexible Space Solar Arrays, Past, Present and Future," *2018 IEEE 7th World Conference on Photovoltaic Energy Conversion (WCPEC) (A Joint Conference of 45th IEEE PVSC, 28th PVSEC & 34th EU PVSEC)*, 2018, pp. 3530–3534, 10.1109/PVSC.2018.8547918.

[3] J. Sun, "A New Design of the 3D Deployable Solar Array in the Aerospace Field and Kinematic Analysis during Deployment," *Journal of Physics: Conference Series*, Vol. 2364, nov 2022, p. 012039, 10.1088/1742-6596/2364/1/012039.

[4] J. Parker, F. Hameli, J. Knittel, M. Caudill, S. Chikine, S. Baskar, A. Koehler, and P. Imler, "AAS 24-064 The Preliminary Mission Design of the Emirates Mission to Explore the Asteroids (EMA)," 02 2024.

[5] R. Calaon, C. Allard, and H. Schaub, "Solar Electric Propulsion GN&C Pointing State Overview For The Emirates Mission To The Asteroid Belt," *AAS Guidance and Control Conference*, Breckenridge, CO, Feb. 2–7 2024. Paper No. AAS 24-056.

[6] L. Kiner, C. Allard, and H. Schaub, "Two-Axis Gimbal Simulation Overview For The Emirates Mission To The Asteroid Belt," *AAS Guidance, Navigation and Control Conference*, Breckenridge, CO, Jan. 31 – Feb. 5 2025. Paper No. AAS-25-013.

[7] A. Cheng, J. Atchison, B. Kantsiper, A. Rivkin, A. Stickle, C. Reed, A. Galvez, I. Carnelli, P. Michel, and S. Ulamec, "Asteroid Impact and Deflection Assessment mission," *Acta Astronautica*, Vol. 115, 2015, pp. 262–269.

[8] M. K. Chamberlain, S. H. Kiefer, M. LaPointe, and P. LaCorte, "On-orbit flight testing of the Roll-Out Solar Array," *Acta Astronautica*, Vol. 179, 2021, pp. 407–414.

[9] A. Trebi-Ollennu, W. Kim, K. Ali, O. Khan, C. Sorice, P. Bailey, J. Umland, R. Bonitz, C. Ciarleglio, J. Knight, N. Haddad, K. Klein, S. Nowak, D. Klein, N. Onufer, K. Glazebrook, B. Kobeissi, E. Baez, F. Sarkissian, M. Badalian, H. Abarca, R. G. Deen, J. Yen, S. Myint, J. Maki, A. Pourangi, J. Grinblat, B. Bone, N. Warner, J. Singer, J. Ervin, and J. Lin, "InSight Mars Lander Robotics Instrument Deployment System," *Space Science Reviews*, Vol. 214, No. 5, 2018, p. 93.

[10] M. Robinson, C. Collins, P. Leger, W. Kim, J. Carsten, V. Tompkins, A. Trebi-Ollennu, and B. Florow, "Test and validation of the Mars Science Laboratory Robotic Arm," *2013 8th International Conference on System of Systems Engineering*, 2013, pp. 184–189, 10.1109/SYSoSE.2013.6575264.

[11] V. Verma, J. Carsten, and S. Kuhn, "The evolution of the curiosity rover sampling chain," *Journal of Field Robotics*, Vol. 37, No. 5, 2020, pp. 729–753.

[12] H. Schaub and J. L. Junkins, *Analytical Mechanics of Space Systems*. Reston, Virginia: American Institute of Aeronautics and Astronautics, Inc., 4 ed., 2018.

[13] M. J. Sidi, *Spacecraft Dynamics and Control: A Practical Engineering Approach*, Vol. 7. Cambridge University Press, 1997.

[14] C. Allard, M. D. Ramos, H. Schaub, P. Kenneally, and S. Piggott, "Modular Software Architecture for Fully Coupled Spacecraft Simulations," *Journal of Aerospace Information Systems*, Vol. 15, No. 12, 2018, pp. 670–683.

[15] P. W. Kenneally, S. Piggott, and H. Schaub, "Basilisk: A Flexible, Scalable and Modular Astrodynamics Simulation Framework," *Journal of Aerospace Information Systems*, Vol. 17, Sept. 2020, pp. 496–507.

[16] J. Vaz Carneiro and H. Schaub, "Spacecraft Dynamics With The Backsubstitution Method: Survey And Capabilities," *AAS Spaceflight Mechanics Meeting*, Kauai, Hawaii, Jan. 19–23 2025. Paper No. AAS 25-232.

[17] C. Allard, M. D. Ramos, and H. Schaub, "Computational Performance of Complex Spacecraft Simulations Using Back-Substitution," *Journal of Aerospace Information Systems*, Vol. 16, No. 10, 2019, pp. 427–436.

[18] J. Vaz Carneiro, C. Allard, and H. Schaub, "General Dynamics for Single- and Dual-Axis Rotating Rigid Spacecraft Components," *Journal of Spacecraft and Rockets*, Vol. 61, July–August 2024, pp. 1099–1113, 10.2514/1.A35865.

[19] L. Kiner, H. Schaub, and C. Allard, "Spacecraft Backsubstitution Dynamics with General Multibody Prescribed Subcomponents," *Journal of Aerospace Information Systems*, Vol. 0, No. 0, 0, pp. 1–13, doi:10.2514/1.I011491.

[20] C. Allard, H. Schaub, and S. Piggott, "General Hinged Rigid-Body Dynamics Approximating First-Order Spacecraft Solar Panel Flexing," *Journal of Spacecraft and Rockets*, Vol. 55, No. 5, 2018, pp. 1290–1298.

[21] J. Alcorn, C. Allard, and H. Schaub, "Fully Coupled Reaction Wheel Static and Dynamic Imbalance for Spacecraft Jitter Modeling," *AIAA Journal of Guidance, Control, and Dynamics*, Vol. 41, No. 6, 2018, pp. 1380–1388, 10.2514/1.G003277.

[22] J. Alcorn, C. Allard, and H. Schaub, "Fully-Coupled Dynamical Jitter Modeling Of Variable-Speed Control Moment Gyroscopes," *AAS/AIAA Astrodynamics Specialist Conference*, Stevenson, WA, Aug. 20–24 2017. Paper No. AAS-17-730.

[23] C. Allard, M. Diaz-Ramos, and H. Schaub, "Spacecraft Dynamics Integrating Hinged Solar Panels and Lumped-Mass Fuel Slosh Model," *AIAA/AAS Astrodynamics Specialist Conference*, Long Beach, CA, Sept. 12–15 2016.

[24] J. Vaz Carneiro, C. Allard, and H. Schaub, "Effector Dynamics For Sequentially Rotating Rigid Body Spacecraft Components," *AAS/AIAA Astrodynamics Specialist Conference*, Big Sky, MO, Aug. 13–17 2023. Paper AAS 23–192.

[25] J. Vaz Carneiro, P. Johnson, and H. Schaub, "Backsubstitution Method For Spacecraft With Generally Translating Appendages," *AAS Astrodynamics Specialist Conference*, Broomfield, CO, Aug. 11–15 2024. Paper No. AAS 24-248.

[26] C. Allard, J. Maxwell, and H. Schaub, "A Transport Theorem for the Inertia Tensor for Simplified Spacecraft Dynamics Development," International Astronautical Conference, Paris, France, Sept. 18-22, 2022.